



---

**Universidad de Valladolid**

**FACULTAD DE CIENCIAS**

**TRABAJO FIN DE GRADO**

**Grado en química**

**COSMO-SAC study of electrolytes for battery application**

**Autor/a: Álvaro De La Fuente Villanueva**

**Tutor/es/as: María Carmen Barrientos Benito,  
Sondre Kvalvåg Schnell**

**Año: 2023**

# Preface

This project is made as a specialization course in materials technology TMT4500 at the Norwegian university of science and technology (NTNU), and later presented as a bachelor's thesis at Universidad de Valladolid (Uva). I would like to acknowledge my supervisor Sondre for helping me with the problems and the project as well as my family and friends for the emotional support.

# Abstract

In this project, we use a semi-empirical quantum chemistry method named COSMO-SAC for evaluating the activity coefficients and the Gibbs free energy of mixing of the most common organic solvent binary mixtures used in Lithium-ion batteries. These are made of four carbonic acid derivatives: dimethyl carbonate (DMC), diethyl carbonate (DEC), ethylene carbonate (EC) and propylene carbonate (PC). A DFT study prior to the use of COSMO-SAC was performed, emphasizing on vibrational analysis and electrostatic potential surface mapping. Activity coefficients are studied at different conditions of temperature, composition, and mole fraction. Both excess free energy and free energy of mixing are also studied. The results fulfil the expected behaviours, but they are not precise. For some specific conditions of temperature and concentration, the model is not suitable.

# Resumen

En este trabajo, se ha utilizado un método semi-empírico mecanocuántico denominado COSMO-SAC para evaluar los coeficientes de actividad y energías libres de mezcla para las mezclas binarias más comunes en baterías de ión-litio. Éstas están constituidas por derivados del ácido carbónico: carbonato de dimetilo (DMC), carbonato de dietilo (DEC), carbonato de etileno (EC) y carbonato de propileno (PC). Se realizó un estudio DFT previo al uso de COSMO-SAC, enfatizado en análisis vibracional y mapeado de superficies de potencial electrostático. Los coeficientes de actividad fueron estudiados a diferentes condiciones de temperatura, composición y fracción molar. Ambas energías libres (exceso y mezcla) fueron estudiadas también. Los resultados son afines con lo esperado, pero no son precisos. Para algunas condiciones de temperatura y concentración, el modelo no es aplicable.

# Index

<b>1. Introduction</b>	<b>5</b>
1.1. Background and motivation	5
1.1.1. Batteries	5
1.1.2. Predictive models	6
<b>2. Objectives</b>	<b>7</b>
<b>3. Theory</b>	<b>9</b>
3.1. Density functional theory (DFT)	9
3.1.1. Method description	10
3.1.2. DFT functionals	11
3.1.3. Basis sets	12
3.1.4. Optimization and vibrational analysis	13
3.2. Sigma profile plotting	14
3.3. Splitting the sigma profile contributions	16
3.4. COSMO-SAC 2002 for activity coefficients	16
3.5. COSMO-SAC 2010 for activity coefficients	19
3.6. Dispersive interactions	20
<b>4. Method</b>	<b>22</b>
4.1. Databases	22
4.2. Implementation of the code	22
4.3. Activity coefficients	23
4.4. Excess Gibbs free energy	23
<b>5. Results and discussions</b>	<b>25</b>
5.1. DFT results	25
5.1.1. Energy calculation	25
5.1.2. Optimized geometry	26
5.1.3. Infrared spectra	26
5.1.4. Electrostatic potential	27
5.2. Activity coefficients	27
5.2.1. Composition	27
5.2.2. Temperature dependence	28
5.2.3. Components dependence	29
5.3. Gibbs free energy of mixing	30
<b>6. Conclusion</b>	<b>32</b>
<b>7. Further work</b>	<b>33</b>
<b>8. References</b>	<b>34</b>
<b>9. Appendices</b>	<b>37</b>
Appendix A: Activity coefficient profiles	37
Appendix B: Excess free energy of mixing	41
Appendix C: Gibbs free energy of mixing	44
Appendix D: Infrared vibrational spectra	48
Appendix E: Electrostatic potential surfaces	50

# List of figures and tables

*Table 1. Structure and relevant properties (dielectric constant  $\epsilon$  and viscosity  $\eta$ ) of carbonic acid esters for battery applications.*

*Table 2. Parameters for COSMO-SAC 2002*

*Table 3. Parameters for COSMO-SAC 2010 and their values.*

*Table 4. Values of  $\epsilon_i / K_b$  for different atoms and hybridizations in COSMO-SAC-dsp*

*Table 5. Identifiers for carbonate esters.*

*Table 6: Energies calculated using DFT theory with different functionals and basis for the minimum energy conformer.*

*Table 7: Ratio of excess free energy in equimolar mixtures.*

*Figure 1. Sigma profile  $p\sigma$  for DMC (616-49-1) and DEC (96-49-1) in both databases*

*Figure 2. Temperature dependence of  $\ln(\gamma)$  for three mixtures of DMC and DEC.*

*Figure 3. Activity coefficients map for different mixtures containing EC at 303K*

# 1. Introduction

## 1.1. Background and motivation

### 1.1.1 Batteries

In these coming years, the need for new batteries is in rise. The energetic demand is increasing way faster than the research in new and more sustainable ways of producing and storing it. For this reason, there is some research in batteries now focusing on developing new ones based on, for example, Al-ion instead. Aluminium is one of the most common elements in earth crust, and its obtaining method is widely studied and improved each year. Potassium batteries are also growing interest since it is chemically similar to Li, has a lower reduction potential, and is more abundant and easier to refine. However, the dominance of Li-ion batteries (LIB) will go on for several years from now<sup>i</sup>.

Li-ion batteries are, undoubtedly, the most used batteries throughout the world mainly because of their high charge density. LIB are capable of storing enormous amounts of energy in a compact and light device. Some other advantages are the low self-discharge rate, which would mean an efficiency loss, and the good cycle life, which means that they work properly after many cycles of charge-discharge.

Their usage is being studied not only for improving electronic devices such as laptops, mobile phones etc., but also, for electric vehicles.

Research in LIB is nowadays focused in perfecting the three parts of the battery [23]:

- The anode, by changing its composition from graphene to Li alloys with tin or silicon that present a higher capacity.
- The cathode, by using other Li oxides such as the lithium-nickel-manganese oxide (LNMO).
- The electrolyte, by using polymers, gel, or solid-state electrolytes as well as ionic liquids.

One of the biggest problems of LIB is the recycling process [30]. The most used electrolytes are made of a Li salt such as LiPF<sub>6</sub> (lithium hexafluorophosphate), LiTFSI (Lithium bis(trifluoromethane sulfonyl) imide), etc., dissolved in an organic solvent with additives. This organic solvent is a mixture of carbonic acid esters. These chemicals are toxic, volatile and may decompose by thermal decomposition or reacting with air and water, consequently generating formaldehyde, acetaldehyde, ethanol, methanol, or formic acid [28].

All the points covered above are time consuming, so the usage of predictive models might be a solution to this problem.

### 1.1.2 Predictive models

Predictive models are growing massive interest by not only research groups, but also the chemical industry for several reasons. Some of them being not needing to buy the compounds for studying their properties, the lack of risk involved in these measurements, time saving, free software for academic purposes in general and accuracy in the obtained data.

COSMO-SAC (Conductor-like Screening Model for segment activity coefficients) is, without doubt, a useful and promising tool. Activity coefficients are truly versatile for refining thermodynamic properties of real mixtures. Many other properties can be obtained e.g., vapour-liquid equilibrium, solubility [10] [24], partition coefficients, viscosity, enthalpy of mixture [16] [21] etc.

## 2. Objectives

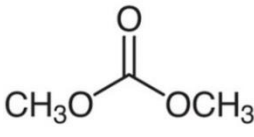
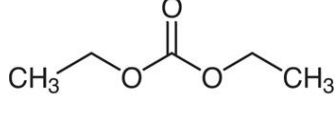
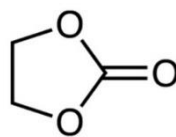
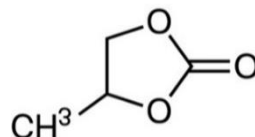
The main problem resides in the need of an electrolytic mixture that presents some qualities: being a one-phase liquid at room temperature, being able to dissolve the ion, enabling its transport between the electrodes, thermal stability etc. This search would take years of trying and repeating mixtures with different components, so we decided to use a computer software called COSMO-SAC[4]. This tool predicts different thermodynamical properties such as activity coefficients, liquid-vapor phase equilibrium etc. by studying the charge density of fragments of the molecules using quantum chemical methods.

Both variants: COSMO-SAC (conductor-like screening model-segment activity coefficient, created by Lin and Sandler [4]) and COSMO-RS (conductor-like screening model for real solvents, created by Klam et al.[1]) have been used throughout the last years for different purposes such as drug development, industrial modelling for new materials etc., but we will now use an adapted version for electrolytes called eCOSMO-SAC [12] (electrolyte conductor-like screening model-segment activity coefficient).

The focus of this work is to study some properties of the most used electrolytic solvents present in lithium batteries. These are carbonic acid esters [25]. In general, they present a high permittivity and there are two types: cyclic and linear. The first ones dissolve Li salts such as LiTFSI and LiPF<sub>6</sub>, and the second ones add fluidity to the solution (the cyclic esters have a really high viscosity which is an inconvenience because it implies a loss of efficiency). A good mixture of solvents should be able to provide an efficient transport of Li ions between the cathode and anode [11] [13].

The components to be studied are ethylene carbonate (EC), propylene carbonate (PC), dimethyl carbonate (DMC) and diethyl carbonate (DEC). (See table 1 below)

Table 1. Structure and relevant properties (dielectric constant  $\epsilon$  and viscosity  $\eta$ ) of carbonic acid esters for battery applications.

	DMC	DEC	EC	PC
Structure				
Cyclicity	Linear	Linear	Cyclic	Cyclic
$T_m$ (K)**	278.2	198.2	311.2	220.3
$T_b$ (K)**	363.5	400	516.7	513.2
$\epsilon$	3.107	2.805	89.78	64.92
$\eta$ (mPa-s)	0.59	0.75	1.93	2.52

\*These values were obtained experimentally by Lide [31]

\*\*These values were obtained in the NIST online database [14]

By doing this, the applicability of COSMO-SAC in battery research will be studied as well as give some data on these electrolytic mixtures for a future enhancement or development of a solvent for a new battery.

In addition, in this study, we have performed a theoretical study within the Density Functional Theory (DFT) context for the ground-level energy of the four molecules (ethylene carbonate (EC), propylene carbonate (PC), dimethyl carbonate (DMC) and diethyl carbonate (DEC)), as well as a vibrational frequency study.



## 3. Theory

To carry out this study we are using COSMO-SAC. Both COSMO models, COSMO-RS (real solvent) and COSMO-SAC are based on UNIFAC [19] [16] (semi-empirical method for activity coefficients calculation): instead of using interactions between the different functional groups of a molecule to describe the properties of a real mixture, it rather considers interactions between several segments of constant charge density. Using the different data given by these segments, we are able to calculate the activity coefficients of a specific mixture of components. It is also possible to study the properties of ionic liquids [17] [26] and electrolytes combining it with the Pitzer-Debye-Hückel model [12].

This requires a density functional theory (DFT) calculation to obtain these segments and their respective charge density. Specifically, Dmol<sup>3</sup>, Gaussian and GAMESS software are used for this purpose.

The DFT calculations must perform the following steps:

- Set a fixed location for all the nuclei.
- Divide the molecule in segments of different electronic density.
- Calculate the surface area and volume of the molecule and the different segments.
- Define the position of the segments as well as their charge density.

In COSMO-SAC-2010, the program also considers which segment is related to a hydrogen-bonding atom, thus classifying them into three groups (see 3.5):

- Not hydrogen-bonding atom (NHB).
- OH: the atom correlated to the segment is either an O or H atom.
- OT: the atom is N, F, H (bonded to F or N) or O not bonded to H.

### 3.1. Density functional theory (DFT)

Density functional theory is one of the most used computational procedures applied to chemistry. The method is based on the assumption that the electronic energy of a molecule can be described using a function that accounts for the electron probability density ( $\rho$ ) and depends on the point of space that is being studied ( $r$ ). Therefore, the energy is treated as a functional of this electron density function. This is written as  $E[\rho(r)]$ .

DFT is not only useful because it accounts for the correlation energy, but also because the use of only one function is necessary for a N-electron molecule without adding constraints.

### 3.1.1. Method description

The starting point of DFT are the Hohenberg-Kohn existence theorem [32], which states that the electronic ground state energy can be written as a functional of the electron density and an external potential. This leads to the statement that ground-state electronic properties are determined by electron density.

$$E[\rho] = T[\rho] + V_{ee}[\rho] + \int \rho(r)v(r)dr = E_{HK}[\rho] + \int \rho(r)v(r)dr \quad (1)$$

Here,  $T$  is the kinetic energy,  $V_{ee}$  is the potential energy between electrons,  $v(r)$  is the external potential that depends on the point of space and  $E_{HK}[\rho]$  is the Hohenberg-Kohn energy.

After proving the previous theorem, P. Hohenberg and W. Kohn modelled an adapted version of the variational principle. This is the Hohenberg-Kohn variational theorem. The procedure is similar to the variational principle, so we know that a variation under a constraint is a minimum, however, in this case, we vary the energy, and the constraint is set to be that the number of electrons (the integral of the electron density over space) is constant. Then, the expression by using the Langrange multiplier ( $\mu$ ) would be as follows:

$$\delta \left\{ E[\rho] - \mu \int \rho(r)dr \right\} = 0 \quad (2)$$

After inserting equation (1), we get the fundamental equation for DFT:

$$\mu = \frac{\delta E_{HK}[\rho]}{\delta \rho(r)} + v(r) \quad (3)$$

Some years later, W. Kohn and L.J. Sham rewrote equation (1) to generate solvable equations by using a reference system with the same electron density as the system of interest. After some derivation, the functional looks as follows:

$$E[\rho] = T_{ref}[\rho] + J[\rho] + E_{XC}[\rho] + \int \rho(r)v(r)dr \quad (4)$$

$J[\rho]$  is the pairwise potential between electrons and  $E_{XC}[\rho]$  is called exchange-correlation energy and the expression for it is:

$$E_{XC}[\rho] = T[\rho] + V_{ee}[\rho] - (T_{ref}[\rho] + J[\rho]) \quad (5)$$

Inserting equation (4) in equation (3), gives us the following expression:

$$\mu = \frac{\delta T_{ref}[\rho]}{\delta \rho(r)} + \frac{\delta J[\rho]}{\delta \rho(r)} + \frac{\delta E_{XC}[\rho]}{\delta \rho(r)} + v(r) = \frac{\delta T_{ref}[\rho]}{\delta \rho(r)} + v_{eff}(r) \quad (6)$$

The last term in the equation above, is the effective potential. The main idea behind this is that the electrons in our system behave identically as they do in the reference system

when moving in an effective potential. Therefore, we can formulate an eigenvalue equation using the expanded form of the effective potential: The Kohn-Sham equation.

$$\left\{ h_1 + j_0 \int \frac{\rho(r_2)}{|r_1 - r_2|} dr_2 + v_{xc}(r_1) \right\} \psi_m^{KS}(r_1) = \varepsilon_m^{KS} \psi_m^{KS}(r_1) \quad (7)$$

Where  $h_1$  is the one-electron operator,  $j_0 = \frac{e^2}{4\pi\epsilon_0}$ ,  $v_{xc}(r_1) = \frac{\delta E_{xc}[\rho]}{\delta \rho(r)}$  and  $\psi_m^{KS}(r_1), \varepsilon_m^{KS}$  are the Kohn-Sham orbitals and energy.

$E_{xc}[\rho]$  is often expressed as a sum of exchange and correlation energies.

To solve the Kohn-Sham equation, we use a self-consistent field method in which the KS orbitals are optimized until convergence.

### 3.1.2. DFT functionals

The problem with the Kohn-Sham equation is the search for a suitable form of the exchange-correlation functional that yields the best results in our calculations. Several approaches have been used such as local density approximations (LDA), generalized-gradient approximation (GGA) and hybrid functionals.

- LDA is the most basic functional. It is often derived using the Thomas-Fermi-Dirac method and states that the exchange-correlation term depends only on the local electron density. Some improved versions are the Perdew-Zunger (PZ) LDA, Ceperley-Alder (CA) LDA, Vosko-Wilk-Nusair (VWN) LDA etc.
- GGA in contrast to LDA, describes the exchange-correlation functional as gradient-dependent instead of point-dependent. The general expression is:  $E_{xc}[\rho] = \int f(\rho(r), \nabla\rho(r)) dr$ . The most famous GGA functionals are the Perdew-Burke-Ernzerhof (PBE) and revised Perdew-Burke-Ernzerhof (RPBE).
- Hybrid functionals are made by empirically optimizing a linear combination of contributions to exchange and correlation from different sources. Such contributions could be i.e., Hartree-Fock exchange, Møller-Plesset second order perturbation theory correlation, etc. These are the most accurate, and therefore utilized, functionals. Among them, Becke's three-parameter exchange with Lee-Yang-Parr correlation (B3LYP) [37][38] and B2PLYPD3 [39][40] are the most outstanding ones. B3LYP is made up of a LDA term for local effects on the exchange-correlation, a Becke exchange term (B88) that itself is a combination of HF and GGA exchange, and, lastly, the LYP correlation energy and spin density. In B2PLYP, the energy functional is a linear combination of GGA exchange and correlation terms (same as in B-LYP methods), HF exchange and MP2 correlation.

To deal with weak dispersion interactions, we have used the double hybrid density functional B2PLYP with explicit dispersion correction B2PLYP-D3. This correction adds the D3 version of Grimme's dispersion with the original D3 damping function [42].

### 3.1.3. Basis sets

In 3.1.1, we defined the Kohn-Sham equation and mentioned that we must solve it using the self-consistent field approach. This consists of optimizing the orbital coefficients that generate molecular orbitals, using the linear combination of atomic orbitals (LCAO), until convergence is achieved (this means that the orbital coefficients used to compute the integrals for the operators are the same as the ones that we get out from the SCF process). However, in order to set up this method, we need a feasible description of the atomic orbitals. This task is not trivial, and many authors have been developing new ones since the invention of the method. These are the so-called *basis sets*.

The initial approach was to use Slater-type orbitals (STO), which are constructed using spherical harmonics ( $Y_{l,m_l}$ ), and radial distribution functions that depend on the effective charge and principal quantum number:

$$\psi_{n,l,m_l}(r, \theta, \varphi) = N r^{n_{eff}-1} e^{-\zeta r} Y_{l,m_l}(\theta, \varphi) \quad (8)$$

In the equation above,  $n_{eff}$  is the effective principal quantum number and  $\zeta$  (zeta) is a constant term that depends on the effective nuclear charge. However, these functions failed to correctly describe molecules with more than 3 atoms.

The solution to these problems, introduced some years later, is the use of Gaussian-type orbitals (GTOs). This is because, by multiplying Gaussian functions, it is possible to generate a new Gaussian that is centred between them, and so, being able to generate a proper radial function. One issue with it is that they failed in describing the orbitals close to the nuclei. So instead, contracted Gaussian functions are used. These are linear combination of primitive Gaussian functions centred on the same atom. The use of these basis sets is favourable because they also reduce the computational cost of calculations. One method for obtaining GTOs is to perform a least squares method with the STOs previously optimized in a SCF calculation. These are the STO- $N_g$ G basis (with  $N_g$  being the number of primitive Gaussians). It is also possible to have more precise results by the introduction of double, triple... zeta basis in which the minimal basis for every atom is doubled or tripled respectively. Apart from this, polarization functions can also be added.

Among the most widely used basis sets, we find the Dunning cc-pvNZ basis [33][34][36], which stands for correlation consistent polarized valence-only N-  $\zeta$  (zeta) basis set. As

the name indicates, they have been made up of polarized functions. Diffuse functions can be added to better describe molecular properties.

Worth mentioning due to their importance are the People [34][35] split-valence basis sets, which made a differentiation between the core orbitals and the valence-shell orbitals that play an important role in reactions and molecular properties. They are named X-YZg where X is the number of primitives that are combined the core orbitals' contracted gaussian, Y and Z are the number of primitives in the two contracted Gaussians used in the valence shell. Polarization functions (represented as: \*) can be added too.

The choice of a correct basis set is not trivial and involves the use of several to compare them to achieve a more accurate result.

In the present work, three basis and two functionals were used, these being respectively: 6-31G, 6-311G and aug-cc-pVTZ (the basis sets), B3LYP and B2PLYPD3 (the functionals).

### 3.1.4. Optimization and vibrational analysis

In order to get better results, a geometry optimization is performed using the Berny algorithm implemented in Gaussian16 [41]. The main idea behind this algorithm is to compute analytical derivatives of the surface potential energy until a minimum (or maximum) is found. These derivatives are gradients and Hessians: first and second derivative matrices of energy with respect to geometrical parameters.

The main steps are:

1. Draw the molecule and compute the Hessian, gradient and energy with a force field.
2. Minimize between the previous best fit and the new point after a step.
3. Update the Hessian matrix.
4. Take a step with the Hessian.
5. Check whether the convergence criteria is satisfied. This is done by comparing the maximum and root mean squared forces and displacement with a threshold.
6. If the convergence criteria is fulfilled, the optimization is finished. Otherwise, update the geometry and start again by calculating the energy and gradient.

After the geometry optimization, a vibrational frequency calculation is performed. This order is necessary because normal modes are defined as vibrations in the minimum energy state. Vibrational frequencies in the IR spectra are calculated by computing the mass-weighted Hessian for the minimum energy geometry. This is done by solving the eigenvalue equation (9):

$$\sum_{j=1}^{3N} H_{ij}^{mw} q_j = \omega_i^2 q_i \quad (9)$$

Where  $H_{ij}^{mw}$  is the mass weighted Hessian summed over all atoms (N),  $q_{j/i}$  are the mass weighted cartesian coordinates and the eigenvalues ( $\omega_i^2$ ) are the normal mode frequencies.

## 3.2. Sigma profile plotting

Plotting the sigma profile is the second step in COSMO-SAC. By doing this, a two-dimensional graph that describes the charge density distribution around the different segments of the molecule is generated [18].

To do this, the first step is to calculate the average charge density of the molecule, using the equation proposed by Klamt et al. for COSMO-RS [1]:

$$\sigma_m = \frac{\sum_n \sigma_n^* \frac{r_{ave}^2 r_n^2}{r_{ave}^2 + r_n^2} \exp\left(-\frac{d_{nm}^2}{r_{ave}^2 + r_n^2}\right)}{\sum_n \frac{r_{ave}^2 r_n^2}{r_{ave}^2 + r_n^2} \exp\left(-\frac{d_{nm}^2}{r_{ave}^2 + r_n^2}\right)} \quad (10)$$

Where  $r_{ave}$  was given a value of  $0.5\text{\AA}$ ,  $\sigma_n^*$  is the charge density of segment n in elemental charge (e) unit,  $r_n$  is the segment radius (calculated by eq. (11)) and  $d_{nm}$  is the distance between two segments (calculated by eq. (12)).

$$r_n = \left(\frac{A_n}{\pi}\right)^{0.5} \quad (11)$$

$$d_{mn} = \sqrt{(x_m - x_n)^2 + (y_m - y_n)^2 + (z_m - z_n)^2} \quad (12)$$

$A_n$  is the surface area of segment n.

Equation (10) was updated by Lin and Sandler [2] as follows:

$$\sigma_m = \frac{\sum_n \sigma_n^* \frac{r_{ave}^2 r_n^2}{r_{eff}^2 + r_n^2} \exp\left(-f_{decay} \frac{d_{nm}^2}{r_{eff}^2 + r_n^2}\right)}{\sum_n \frac{r_{ave}^2 r_n^2}{r_{eff}^2 + r_n^2} \exp\left(-f_{decay} \frac{d_{nm}^2}{r_{eff}^2 + r_n^2}\right)} \quad (13)$$

Being  $r_{eff} = (a_{eff}/\pi)^{0.5}$  and  $f_{decay}$  a parameter for dimension scaling (see table 1).

With all this information, a so called sigma profile ( $p(\sigma_n^*)$ ) can be calculated, defined as the probability of finding a segment with a specific charge density  $\sigma_m$ :

$$p(\sigma_m) = \frac{n(\sigma_m)}{\sum_m n(\sigma_m)} = \frac{A(\sigma_m)}{\sum_m A(\sigma_m)} \quad (14)$$

Where  $n(\sigma_m)$  is the number of segments with charge density  $\sigma_m$  and  $A(\sigma_m)$  is the surface area of the segments with charge density equal to  $\sigma_m$ .

After this, the different values of probabilities must be plotted against the calculated charge density values using increments of  $0.001 \text{ e}/\text{\AA}^2$  for a range between  $-0.025$  and  $0.025 \text{ e}/\text{\AA}^2$  (50 intervals).

To generate this, we need a 0-based index for each  $\sigma$  value:

$$i_{left} = \left\lfloor \frac{\sigma - (-0.025 \text{ e}/\text{\AA}^2)}{0.001 \text{ e}/\text{\AA}^2} \right\rfloor \quad (15)$$

The floor bracket defines a mathematical floor function (the function gives back the greatest integer number that is equal or less than the value between brackets).

$$w = \frac{\sigma[i_{left} + 1] - \sigma}{0.001 \text{ e}/\text{\AA}^2} \quad (16)$$

This previous value corresponds to the distance between a certain value of  $\sigma$  and the sides. It is a number between 0 and 1. We can now distribute the segment area between the gridded values of sigma according to the weighting parameter calculated before.

$$p(\sigma)A_i[i_{left}] += wA_n \quad (17)$$

$$p(\sigma)A_i[i_{left} + 1] += (1 - w)A_n \quad (18)$$

By plotting these results against the electronic density grid, we obtain the sigma profile, as shown in Figure 1. Sigma profile  $p(\sigma)$  for DMC (616-49-1) and DEC (96-49-1) in both databases

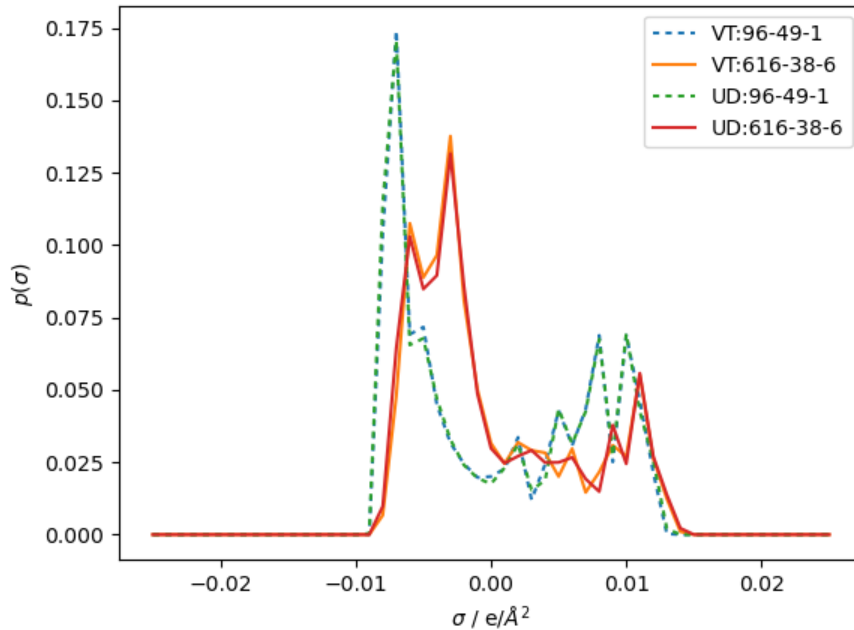


Figure 1. Sigma profile  $p(\sigma)$  for DMC (616-49-1) and DEC (96-49-1) in both databases

### 3.3. Splitting the sigma profile contributions

At this point is where the intermolecular interactions such as hydrogen-bonding should be taken into account according to Lin et al. [3] If this is the case, the corresponding sigma profile can be expressed as an addition of two terms:

$$p(\sigma) = p(\sigma)^{NHB} + p(\sigma)^{HB} \quad (19)$$

Being each of them defined as gaussian functions according to Wang et al. [3]:

$$p(\sigma)^{HB} = 1 - \exp\left(-\frac{\sigma^2}{2\sigma_0^2}\right) \quad (20)$$

Eq. (20) describes the sigma profile of all hydrogen bonding atoms (N, O, F and H) where  $\sigma_0 = 0.007 \text{ e}/\text{\AA}^2$ . Therefore, the different sigma profiles are expressed as it follows:

$$p(\sigma)^{NHB} = \frac{A_i^{NHB}(\sigma)}{A_i} + \frac{A_i^{HB}(\sigma)}{A_i} [1 - p(\sigma)^{HB}] \quad (21)$$

$$p(\sigma)^{OH} = \frac{A_i^{OH}(\sigma)}{A_i} p(\sigma)^{HB} \quad (22)$$

$$p(\sigma)^{OT} = \frac{A_i^{OT}(\sigma)}{A_i} p(\sigma)^{HB} \quad (23)$$

Where  $A_i^{HB} = A_i^{OH} + A_i^{OT}$  is the surface area of all hydrogen-bonding segments and being  $A_i^{OH}$  and  $A_i^{OT}$  the surface areas of hydroxyl groups and the rest of the hydrogen-bonding atoms respectively.

Sigma profiles can usually be found in several databases. In this case we are using two of them: Virginia Tech University and Delaware University and can be reached from different sources [8] [9] [10]. In these databases, a wide variety of sigma profiles for different compounds has been validated and compared to experimental data to be used.

### 3.4. COSMO-SAC 2002 for activity coefficients

Once obtained the sigma profile, the next step is to calculate the natural logarithm of the activity coefficients.



For a mixture of component  $i$  in a solvent  $S$ , the activity coefficient is described by Lin and Sandler [4] as:

$$\ln(\gamma_{i,S}) = \ln(\gamma_{i,S}^c) + \ln(\gamma_{i,S}^r) \quad (24)$$

The first term on the right side is called natural logarithm of the combinatorial activity coefficient and describes the activity coefficient according to the molecular structures of the components in the mixture as follows:

$$\ln(\gamma_{i,S}^c) = \ln\left(\frac{\phi_i}{x_i}\right) + \frac{z}{2} q_i \ln\left(\frac{\theta_i}{\phi_i}\right) + l_i - \frac{\phi_i}{x_i} \sum_j x_j l_j \quad (25)$$

As one can tell, equation (25) is a Staverman-Guggenheim combinatorial term, where the different parameters are calculated as:

$$\theta_i = \frac{x_i q_i}{\sum_j x_j q_j} \quad (26)$$

$$\phi_i = \frac{x_i r_i}{\sum_j x_j r_j} \quad (27)$$

$$l_i = \frac{z}{2}(r_i - q_i) - (r_i - 1) \quad (28)$$

$z$  is the coordination number,  $x_i$  and  $x_j$  are the mole fraction of components  $i$  and  $j$  in the mixture, and:

$$r_i = \frac{V_i}{r_0} \quad (29)$$

$$q_i = \frac{A_i}{q_0} \quad (30)$$

Where  $r_0 = 66.69 \text{ \AA}^3$  and  $q_0 = 79.53 \text{ \AA}^2$  are the normalized values for volume and surface area.

For infinite dilution, the mole fraction of one component is almost equal to 0, making equations (26) and (27) not viable. This results in rewriting them as:

$$\frac{\theta_i}{x_i} = \frac{q_i}{\sum_j x_j q_j} \quad (31)$$

$$\frac{\phi_i}{x_i} = \frac{r_i}{\sum_j x_j r_j} \quad (32)$$

$$\frac{\theta_i}{\phi_i} = \frac{\theta_i/x_i}{\phi_i/x_i} \quad (33)$$

The second term in eq. (24) gives a correction due to the residual activity coefficient generated by the interaction between charge densities of the molecules. According to the authors, this should be calculated as:

$$\ln(\gamma_{i,s}^r) = n_i \sum_{\sigma_m} p_i(\sigma_m) [\ln(\Gamma_s(\sigma_m)) - \ln(\Gamma_i(\sigma_m))] \quad (34)$$

Where  $n_i$  is the number of surface segments with a segment surface area  $a_{eff}$  and can be described as:

$$n_i = \frac{A_i}{a_{eff}} \quad (35)$$

$\sigma_m$  is the screening charge density,  $p_i(\sigma_m)$  is the probability of a segment with a specific screening charge density  $\sigma_m$ , which can be calculated as:

$$p_i(\sigma_m) = \frac{A_i(\sigma_m)}{A_i} \quad (36)$$

and  $\Gamma_s(\sigma_m), \Gamma_i(\sigma_m)$  are the activity coefficients of segment  $m$  in the mixture and in the pure component respectively. These last terms are derived as:

$$\ln(\Gamma_s(\sigma_m)) = -\ln \left\{ \sum_{\sigma_n} p_s(\sigma_n) \Gamma_s(\sigma_n) \exp \left[ -\frac{\Delta W(\sigma_m, \sigma_n)}{RT} \right] \right\} \quad (37)$$

$$\ln(\Gamma_i(\sigma_m)) = -\ln \left\{ \sum_{\sigma_n} p_i(\sigma_n) \Gamma_i(\sigma_n) \exp \left[ -\frac{\Delta W(\sigma_m, \sigma_n)}{RT} \right] \right\} \quad (38)$$

Here, a new term  $\Delta W(\sigma_m, \sigma_n)$  is introduced. This is known as the exchange energy and to calculate it, we use the following expression:

$$\Delta W(\sigma_m, \sigma_n) = \left( \frac{\alpha'}{2} \right) (\sigma_m + \sigma_n)^2 + c_{hb} \max[0, \sigma_{acc} - \sigma_{hb}] \min[0, \sigma_{don} + \sigma_{hb}] \quad (39)$$

The term  $\alpha'$  is the misfit energy of electrostatic interactions,  $c_{hb}$  is a constant and  $\sigma_{hb}$  is the cut-off energy of the hydrogen bonding.  $\sigma_{acc}$  and  $\sigma_{don}$  were described as the maximum and minimum values of  $\sigma_m$  and  $\sigma_n$ .

Table 2. Parameters for COSMO-SAC 2002

Parameter	Value
$\alpha'$	16466.72 Kcal $\text{\AA}^4 \text{mol}^{-1} \text{e}^{-2}$
$c_{hb}$	85580 Kcal $\text{\AA}^4 \text{mol}^{-1} \text{e}^{-2}$
$\sigma_{hb}$	0.0084 $\text{e}\text{\AA}^{-2}$

### 3.5. COSMO-SAC 2010 for activity coefficients

Hsieh et al. [6] proposed modifications in 2010 to make the results for activity coefficients more precise. According to them, the exchange energy should be rewritten as:

$$\Delta W(\sigma_m^t, \sigma_n^s) = c_{ES}(T)(\sigma_m^t + \sigma_n^s)^2 - c_{hb}(\sigma_m^t, \sigma_n^s)(\sigma_m^t - \sigma_n^s)^2 \quad (40)$$

$\sigma_m^t$  and  $\sigma_n^s$  are two different types of sigma profiles, regarding the hydrogen bonding interactions, and the correction term  $c_{ES}$  accounts the electrostatic interactions and is dependent on temperature:

$$c_{ES} = A_{ES} + \frac{B_{ES}}{T^2} \quad (41)$$

The second modification is the division of the hydrogen bonding into the three types mentioned before. The value of  $c_{hb}$  changes depending on the type of hydrogen bonding:

$$c_{hb}(\sigma_m^t, \sigma_n^s) = \begin{cases} c_{OH-OH} & \text{if } s = t = OH \text{ and } \sigma_m^t \sigma_n^s < 0 \\ c_{OH-OT} & \text{if } s = OH, t = OT \text{ and } \sigma_m^t \sigma_n^s < 0 \\ c_{OT-OT} & \text{if } s = t = OT \text{ and } \sigma_m^t \sigma_n^s < 0 \end{cases} \quad (42)$$

And 0 otherwise. Due to this separation, a new term must be added to equation (34):

$$\ln(\gamma_{i,S}^r) = n_i \sum_t^{nhb,OH,OT} \sum_{\sigma_m} p_i^t(\sigma_m^t) \left[ \ln(\Gamma_s^t(\sigma_m^t)) - \ln(\Gamma_i^t(\sigma_m^t)) \right] \quad (43)$$

And thus, equation (37) becomes:

$$\ln(\Gamma_s^t(\sigma_m^t)) = -\ln \left\{ \sum_s^{nhb,OH,OT} \sum_{\sigma_n} p_s^s(\sigma_n^s) \Gamma_s^s(\sigma_n^s) \exp \left[ -\frac{\Delta W(\sigma_m^t, \sigma_n^s)}{RT} \right] \right\} \quad (44)$$

The same change is also used in equation (38).

$$\ln(\Gamma_i^t(\sigma_m^t)) = -\ln \left\{ \sum_i^{nhb,OH,OT} \sum_{\sigma_n} p_i^s(\sigma_n^s) \Gamma_i^s(\sigma_n^s) \exp \left[ -\frac{\Delta W(\sigma_m^t, \sigma_n^s)}{RT} \right] \right\} \quad (45)$$

All the parameters for COSMO-SAC 2010 are implemented in the code as shown in Table 3:

Table 3. Parameters for COSMO-SAC 2010 and their values.

Parameter	Value
$q_0$	79.53 Å <sup>2</sup>
$r_0$	66.69 Å <sup>3</sup>
$z$	10
$a_{\text{eff}}$	7.25 Å <sup>2</sup>
$r_{\text{eff}}$	$(a_{\text{eff}}/\pi)^{0.5}$
$f_{\text{decay}}$	3.57
COH-OH	4013.78 kcal Å <sup>4</sup> mol <sup>-1</sup> e <sup>-2</sup>
COT-OT	932.31 kcal Å <sup>4</sup> mol <sup>-1</sup> e <sup>-2</sup>
COH-OT	3016.43 kcal Å <sup>4</sup> mol <sup>-1</sup> e <sup>-2</sup>
$\sigma_0$	0.007 e Å <sup>-2</sup>
$A_{\text{ES}}$	6525.69 kcal Å <sup>4</sup> mol <sup>-1</sup> e <sup>-2</sup>
$B_{\text{ES}}$	1.4859 E8 kcal Å <sup>4</sup> K <sup>2</sup> mol <sup>-1</sup> e <sup>-2</sup>
$N_{\text{A}}$	6.022140758 E23 mol <sup>-1</sup>
$k_{\text{B}}$	1.38064903 E-23 J K <sup>-1</sup>
$R$	4184 kcal mol <sup>-1</sup> K <sup>-1</sup>

### 3.6. Dispersive interactions

Hsieh et al. also considered the interaction between molecules due to dispersive interactions [6]. This way, a new term was added to equation (24):

$$\ln(\gamma_{i,S}) = \ln(\gamma_{i,S}^c) + \ln(\gamma_{i,S}^r) + \ln(\gamma_{i,S}^{dsp}) \quad (46)$$

The combinatorial and residual terms are calculated the same way. However, the new contribution to the activity coefficient is slightly different:

$$\ln(\gamma_{i,S}^{dsp}) = Ax_i^2 \quad (47)$$

Where A is a parameter calculated as follows:

$$A = w \left[ 0.5 \left( \frac{\varepsilon_1}{k_b} + \frac{\varepsilon_2}{k_b} \right) - \sqrt{\frac{\varepsilon_1}{k_b} \frac{\varepsilon_2}{k_b}} \right] \quad (48)$$

$k_b$  is the Boltzmann's constant and  $\varepsilon_i$  is the dispersion parameter which has different values for different atoms (see Table 4) and their values are obtained from experimental data.

$w$  can take different values according to the functional groups in the molecule:

$$w = \begin{cases} -0.27027 \text{ K}^{-1} & \text{if water + hb - only acceptor} \\ -0.27027 \text{ K}^{-1} & \text{if COOH + (nhb or hb - donor and acceptor)} \\ -0.27027 \text{ K}^{-1} & \text{if water + COOH} \\ 0.27027 \text{ K}^{-1} & \text{otherwise} \end{cases} \quad (49)$$

COOH refers to the carboxyl group, nhb are molecules that cannot make hydrogen bonds, hb-only acceptor are molecules that are only capable of accepting protons from a hb molecule and hb-donor and acceptor, as the name suggests, are molecules that can be both donor and acceptor of protons.

Table 4. Values of  $\varepsilon_i/k_b$  for different atoms and hybridizations in COSMO-SAC-dsp

Atom type	$(\varepsilon_i/k_b) / K$
C (sp <sup>3</sup> )	115.7023
C (sp <sup>2</sup> )	117.4650
C (sp)	66.0691
N (sp <sup>3</sup> )	15.4901
N (sp <sup>2</sup> )	84.6268
N (sp)	109.6621
-O-	95.6184
=O	-11.0549
F	52.9318
Cl	104.2534
H (water)	58.3301
H (OH)	19.3477
H (NH)	141.1709
H (other)	0
Other	Invalid

## 4. Method

### 4.1. Databases

The first step in order to use COSMO-SAC is to generate the sigma profiles. For this purpose, a density functional theory (DFT) calculation must be performed. Authors normally use Dmol<sup>3</sup> because an additional COSMO-based module is added [29]. DFT is a molecular structure dependent method, so the choice of a relevant structure is a crucial step. So, a geometry optimization is also performed by choosing random starting points and minimizing its energy to get a global minimum.

Once obtained the structure, we run the calculations specifying in the input file which parameters we are interested in, this being: surface area, volume, and charge density of the segments. Afterwards, the sigma profile is generated as we mentioned in the theory part.

However, in this work we are not following this process. This is because DFT is a complex and time-consuming method and must be optimized for the specific level of calculation. Instead, we are using two databases developed by two universities: Virginia Tech University (VT) [9] [10] and University of Delaware (UD).

The first one was earlier generated, so the latest upgrade in COSMO-SAC, which corresponds to the dispersive contribution, is not implemented in the code. But VT can be used to calculate activity coefficients for ternary mixtures alike UD.

### 4.2. Implementation of the code

COSMO-SAC is an open-source program, and its code is stored in a git-hub page thanks to Bell et al. [8] <https://github.com/usnistgov/COSMOSAC>, where one can also find some examples on how to make a script. These files are normally written using python.

We paid close attention to the `easy_COSMOSAC.py` example, in which you can set some parameters and get the activity coefficients for a binary or tertiary mixture. These parameters are temperature, mole fraction and identifiers for the components in the mixture (see Table 5). These identifiers can be found in the compound lists for the databases and several of them are implemented (name, CAS number, InChiKey ...), however, a bad choice in the identifiers could lead to a problem, so we chose to use CAS numbers as they are unique for each chemical.

Table 5. Identifiers for carbonate esters.

	DMC	DEC	EC	PC
ID (UD)	325	841	843	487
ID (VT)	1242	704	678	1224
Name (UD)	DIMETHYL_CARBOATE	DIETHYL_CARBOATE	ETHYLENE_CARBOATE	PROPYLENE_CARBOATE
Name (VT)	DIMETHYL-CARBOATE	DIETHYL-CARBOATE	ETHYLENE-CARBOATE	PROPYLENE-CARBOATE
CAS#	616-38-6	105-58-8	96-49-1	108-32-7
SMILES	COC(=O)OC	CCOC(=O)OCC	C1(=O)OCCO1	C1(=O)OC[C@@H](O1)C
INCHIKEY	IEJIGPNLZYLLBP-UHFFFAOYSA-N	OIFBSDVPJOWBCH-UHFFFAOYSA-N	KMTRUDSVKNLOMY-UHFFFAOYSA-N	RUOJZAUFBMNUDX-VKHMHEASA-N

### 4.3. Activity coefficients

The next step is to use the sigma profiles stored in the databases for calculating the activity coefficients using both models: COSMO-SAC 2002 and COSMO-SAC 2010 (dsp).

We should also look at how the activity coefficients depend on the input parameters, these being: temperature, composition, and components in the mixture.

### 4.4. Excess Gibbs free energy

Excess properties are characteristic of non-ideal behaviours. Excess free energy is defined as the extra energy needed to mix two (or more) components. It can be related to the lost work in a mixing process, and this is not optimal for our battery design.

The excess free energy is calculated as follows [7] [15] :

$$G^E = RT \sum_{i=1}^n x_i \ln(\gamma_i) \quad (50)$$

Being  $\gamma_i$  the activity coefficient obtained by COSMO-SAC calculations,  $x_i$  the mole fraction of the component  $i$  in a mixture and  $R$  is the ideal gas constant.

The expression for mixing free energy is:

$$\Delta G_{mix} = \Delta G_{ideal} + \Delta G^E = RT \sum_{i=1}^n x_i \ln(x_i) + x_i \ln(\gamma_i) \quad (51)$$

Note that the first term is always negative or 0 (for the pure component), the consequence of this is that the excess free energy is the property that determines whether the components will mix or de-mix according to the sign: positive  $\Delta G_{mix}$  means de-mixing and negative, the opposite.

By looking at the phase diagrams for these mixtures [22], we are expecting that all of them will mix in liquid state at 303K.



## 5. Results and discussions

### 5.1. DFT results

#### 5.1.1. Energy calculation

In this study, we performed a DFT calculation for the ground-level energy of the four molecules, as well as a vibrational frequency study. For this work, three basis and two functionals were used, these being respectively: 6-31G, 6-311G, aug-cc-pVDZ and aug-cc-pVTZ (the basis sets), B3LYP and B2PLYPD3\* (the functionals).

*Table 6: Energies calculated using DFT theory with different functionals and basis for the minimum energy conformer.*

Molecule	Functional	Basis set	Energy (H)
Ethylene carbonate (EC)	B3LYP	6-31G	-342.268881
		6-311G	-342.36408
		aug-cc-pVTZ	-342.53782
	B2PLYPD3	aug-cc-pVTZ	-342.30516
Propylene carbonate (PC)	B3LYP	6-31G	-381.58185
		6-311G	-381.68532
		aug-cc-pVTZ	-381.8731
	B2PLYPD3	aug-cc-pVTZ	-381.604
Dimethyl carbonate (DMC)	B3LYP	6-31G	-343.48367
		6-311G	-343.58093
		aug-cc-pVTZ	-343.75094
	B2PLYPD3	aug-cc-pVDZ	-343.35471
Diethyl carbonate (DEC)	B3LYP	6-31G	-422.10473
		6-311G	-422.21838
		aug-cc-pVTZ	-422.41755
	B2PLYPD3	aug-cc-pVDZ	-421.90935

The results obtained in the table above were calculated using Gaussian 16\*. In the case of DMC and DEC, we used as geometry input a Z-matrix to force the C<sub>2v</sub> geometry. The reasons for doing this is that we expect this geometry (it looks like there is a rotation axis of 180° and a vertical reflexion plane, both centred in the carbonate group) and that way we solve some calculation problems due to molecular flexibility of the linear species.

B2PLYP/aug-cc-pVTZ level of calculation for DEC and DMC was not possible due to memory requirements, so a lower level was used.

It is not wise to compare these results because the parametrization of the functionals is mostly empirical by comparing to some measurable property (normally thermodynamical like enthalpy or entropy). So, we can only trust the articles in which error measurements are performed. In the article by Grimme S. [40], the performance of the B2PLYP functional is compared with B3LYP. The conclusion is that B2PLYP is more accurate than B3LYP in most cases.

### 5.1.2. Optimized geometry

Another method for comparing the calculation levels is to take, for example, the optimized geometries for EC and PC and look at the optimization parameters (bond lengths, angles and dihedral angles) to see the difference between them.

As a general rule, bond lengths and angles become smaller for higher levels, so for EC and PC, that means a smaller ring. However, in B2PLYP, the double bond between oxygen and carbon is longer. This might be due to the dispersive interactions described by the functional.

### 5.1.3. Infrared spectra

IR spectra can be found in Appendices. For the sake of data overload, only the spectra for B2PLYP/cc-pVTZ (B2PLYP/cc-pVDZ for DEC) will be presented.

The first noticeable characteristics of the spectra are the molar absorption coefficient magnitudes ( $\epsilon$ ). We can see a relation regarding the flexibility of the molecule and the value of  $\epsilon$ . That is why DEC maximum is between 3500 and 4000  $\text{M}^{-1} \text{cm}^{-1}$ , while EC's one is less than 2000  $\text{M}^{-1} \text{cm}^{-1}$ .

By looking at the prominent peaks, we can see two that are common to the four species: one between 1050  $\text{cm}^{-1}$  and 1250  $\text{cm}^{-1}$  that corresponds to the C-O stretch in esters and the clear peak around 1750  $\text{cm}^{-1}$  that is related to the C=O stretch.

DEC and DMC have also a peak that stands out from the rest of the spectra around 1250  $\text{cm}^{-1}$ . This represents one of the normal modes of the hydrocarbon chain in which the hydrogens move forwards and backward simultaneously. This movement is referred to as wagging.

The other peaks represent the fingerprint vibrations of the molecule and are unique for every molecule.

## 5.1.4. Electrostatic potential

In appendix E [9], one can see the electrostatic potential around the molecules. This is related to the electron density around the atoms that set up the molecule. Red parts symbolize the high electrostatic potential, and so, areas where electrophilic species would most probably interact with the molecule. Likewise, green parts symbolize low electrostatic potential, in other words, areas where nucleophilic species would attack.

It is easy to realize, since we only have three different atoms, that charge is concentrated around the oxygen atoms, particularly around the double bonded one.

This electrostatic potential surface is what COSMO-SAC uses to create segments of similar charge density for its future use in activity coefficients calculations.

## 5.2. Activity coefficients

### 5.2.1. Composition

As mentioned, the study is focused on binary mixtures of four carbonic acid esters: DMC, DEC, EC, and PC. This gives six combinations.

The activity coefficients as a function of composition are calculated at 303K and different mole fractions (see Appendices). The choice of temperature is done for relatively common work conditions (Li batteries work in a range between -20–60°C [25])

They all follow the same trend: high mole fraction indicates a low activity coefficient and low mole fraction, the opposite. This is expected because high mole fractions are closer to the ideal conditions of a mixture that corresponds to both components behaving as their pure form.

However, there are three kinds of behaviours regarding the two databases:

- Both describe equally the activity coefficients. This is the case for EC+DEC (A1)
- There is a small displacement between both lines as seen in A2-A4
- The differences are too big to be neglected. This can be seen in A5 and A6

To give a proper explanation, we should look at the differences between the two databases and methods used. In this case, the dispersive interactions were considered in the UD database and not in the VT database because they were not implemented in the code. According to this hypothesis, we can consider that dispersive interactions are mostly relevant for PC+DMC and DMC+DEC. Another reason why EC+DEC activity coefficients are so closely predicted is that their activity coefficients are way higher than the rest, so the differences are not noticeable.

However, some parts of the EC-containing plots are not correct because at high mole fraction of EC, it is no longer a liquid mixture. It becomes a liquid and solid EC at approximately 0.8/0.9 mole fraction of EC.

## 5.2.2. Temperature dependence

Activity coefficients are thermodynamic properties, so they are temperature dependent. We are studying this dependence by choosing a pair of components and changing the temperature in three mixtures of different compositions. We also assume that changes in temperature have the same effect in different mixtures.

We studied the mixture of DMC and DEC at mole fractions 0.2:0.8, 0.5:0.5 and 0.8:0.2 respectively (See figure 2 below).

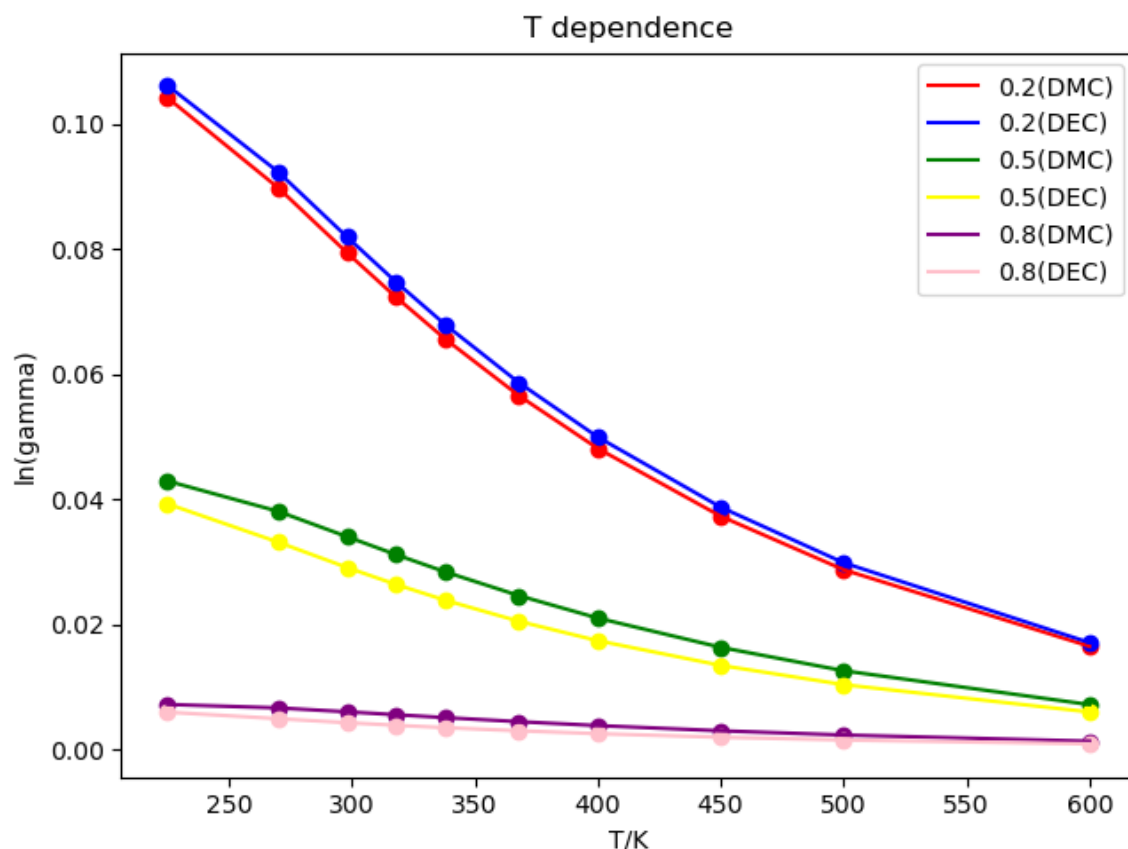


Figure 2. Temperature dependence of  $\ln(\gamma)$  for three mixtures of DMC and DEC.

We can also appreciate here the concentration effect on activity coefficients. It is noticeable that high temperatures decrease the value of  $\ln(\gamma)$ , resulting in a more ideal behaviour. This effect is more evident for low concentrations.

Another important detail to point out here, is that all the lines seem to converge at approximately 700K, however, going further in temperature is not something that we are interested in, since the two components would have already boiled (DMC evaporates at 363K and DEC at 400K), and in these conditions, the battery would not work because there is no fluid phase for the ion transport.

Also, the decrease in activity coefficients becomes smaller at high temperatures, breaking the linearity at low ones.

However, there should be a change in the trend due to phase changes (melting point for DMC is 278.2K and for DEC, 198.2K apart from the previously commented boiling points). The program does not consider these transitions, which is a flaw and could be a future implementation.

### 5.2.3. Components dependence

We shall now look at changes in the activity coefficients when one of the components in the mixture is changed at fixed temperature and mole fraction.

In this case, we chose EC as the non-changing component at three compositions and  $T=303K$ . This is because EC is the most efficient cyclic ester, while the choice between DMC and DEC is still not clear.

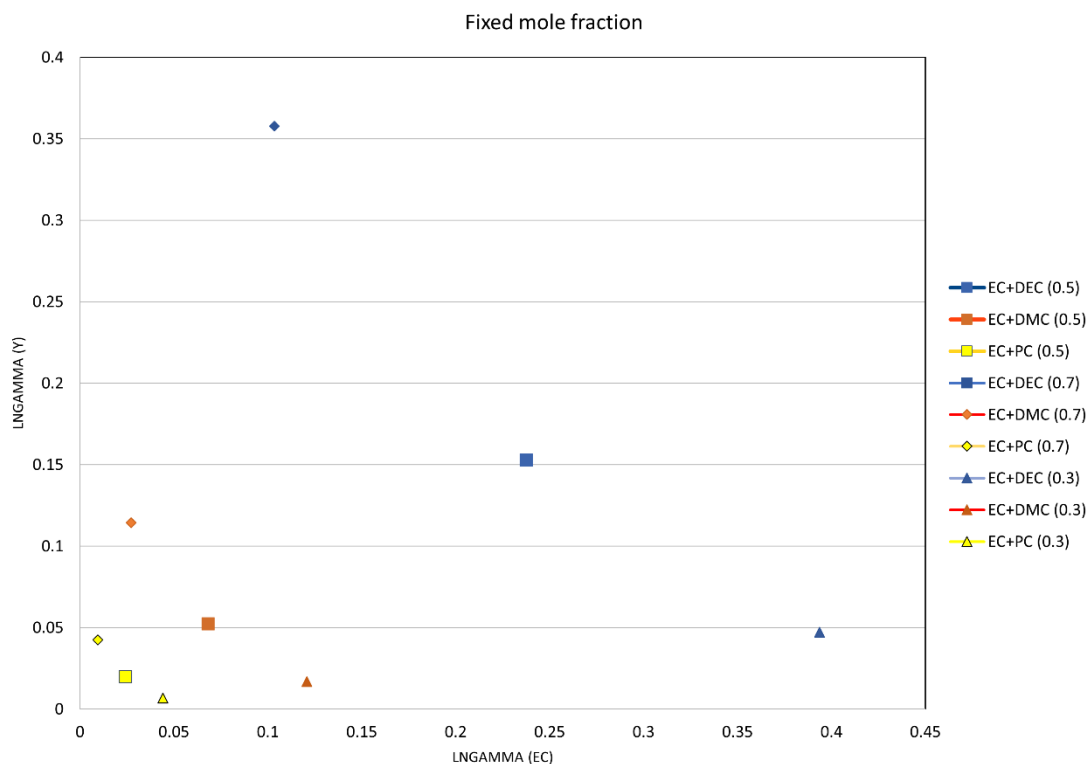


Figure 3. Activity coefficients map for different mixtures containing EC at 303K

We can see that the values at 0.3 mole fraction of EC are higher in the x axis and lower in the y axis. The opposite applies to the 0.7 EC mixture as well. This is an expected behaviour because, as we demonstrated before, higher mole fractions of a component mean lower activity coefficient and vice-versa (see 5.2.1).

With a second look at the plot, we can see that the activity coefficients for both components in the mixture are higher following the pattern DEC >DMC >PC. A possible hypothesis for this is that, since EC and PC are both cyclic esters, their interactions are similar due to its common base structure: the five-atom ring. Meanwhile, its interactions with the linear esters are not ideal, and it looks like these are dependent on the length of the side chains. The longer these chains, the higher the activity coefficient.

Another interesting piece of data that we can obtain with this plot is the positions of the points. If we draw two lines that connect the points for the different mixtures at the same mole fraction, and we calculate their slopes, we can see that at higher percentage of EC in the mixture, both slopes are steeper. This is also connected to the previously explanation, and the reason is that changes of component at high concentrations of EC do not influence  $\ln(\gamma^{EC})$  the same way.

### 5.3. Gibbs free energy of mixing

It is easy to notice by looking at Appendix C, that all the mixtures' free energy profiles follow the same trend: they have a quadratic-like behaviour with higher values (less negative) at higher mole fraction difference, while the lowest free energy is found at equimolar conditions.

To explain this, we can look at the concentration dependence of the mixing free energy contributions in (51):

- The ideal contribution to the free energy is a perfectly symmetric quadratic-like function with its minimum at  $x_i = 0.5$  and negative values between  $-818$  J/mol and  $-1746.14$  J/mol.
- The excess free energy depends on the mixture. In some of them, the maximum is located at  $x_i = 0.5$ , while in others, it is shifted to higher values. However, all of them are positive and have the maximum around the middle part as well. (See Appendix B)

One can interpret this as if the excess free energy is not high enough to change the negative values of the ideal contribution to the free energy of mixing. In de-mixing conditions, such as the ones in a water-hexane mixture for instance, the natural

logarithm of the activity coefficients is considerably higher than these values for carbonic acid esters.

We can also confirm that both databases describe almost equally the mixing free energy.

By comparing the excess free energy with the ideal free energy, we see that, as we mentioned, the excess free energy represents a generally low percentage in the total free energy (Table 7).

*Table 7: Ratio of excess free energy in equimolar mixtures.*

	$\Delta G^E$ (J/mol)	$\Delta G_{ideal}$ (J/mol)*	$ \Delta G^E / \Delta G_{ideal} $
<b>DMC+DEC</b>	77.65703622	-1746.136175	0.0444
<b>EC+DMC</b>	151.7627246	-1746.136175	0.0869
<b>EC+DEC</b>	491.7750613	-1746.136175	0.2823
<b>EC+PC</b>	55.81883354	-1746.136175	0.0320
<b>PC+DMC</b>	26.32044906	-1746.136175	0.0151
<b>PC+DEC</b>	233.1437329	-1746.136175	0.1335

\*  $\Delta G_{ideal}$  is the same for all mixtures and in this case corresponds to  $RT\ln(0.5)$ , being R the ideal gas constant.

The ideal free energy is around 11.5 to 66 times the excess energy, which means that the non-ideal contribution is negligible. However, there are two exceptions: in PC+DEC, the ideal contribution is roughly 7.5 times the excess one, and in EC+DEC, it is 3.5 times the excess free energy. In these cases, the differences are much smaller and should be taken into account when performing other calculations.

By looking at these two cases, we can confirm that the interactions between a cyclic ester and DEC are the furthest ones from ideal behaviour, as one can see in the activity coefficient plots (Appendices).

Also, considering the temperature dependence discussed before, it is clear that, at higher temperatures, the activity coefficients are smaller and thus the free energy is more negative.

After looking in the article by M.S. Ding [20], we can see that the excess free energy predicted by COSMO-SAC differs from the experimental one, meaning that the model is not completely correct, or the sigma profiles are not well generated. Apart from this, in EC+DMC, EC+DEC and EC+PC plots around 0.8/0.9 mole fraction of EC, the phase diagrams predict an overpassing of the liquidus line, which means a solidification of EC.

## 6. Conclusion

In this work, we calculated activity coefficients, an important thermodynamic property that connects the ideal expressions and reality. The non-ideal behaviour is, in some processes, relevant and must be taken into account. We covered the following topics along the project:

- 1 Density functional theory was described and used, as a previous study on the molecules of interest.
- 2 An insight into COSMO-SAC and its working mechanisms was given, as well as some notes on its implementation.
- 3 We generated the activity coefficient plot at 303K and different concentrations for each binary mixture containing carbonic acid esters. Here, we also realized that both databases give back different values for most of the mixtures.
- 4 We had a look at the temperature dependence of the activity coefficients in the DMC+DEC mixture and assumed the same changes with temperature in different mixtures. We could see that phase transitions are not considered by COSMO-SAC.
- 5 The activity coefficient map for two components gave us some information about the interactions between them. In this case, the fixed component was EC due to its high performance in Li batteries. We also saw that changing the mole fraction of EC, has an effect on the differences between components.
- 6 Lastly, we calculated one of the most important properties for an electrolytic solvent: mixing free energy. The results met the experimental calculations as these four components were supposed to mix at 30°C. We came to the conclusion that the non-ideal interactions between carbonic acid esters are, in general, not high enough to make the mixing free energy positive, which means that the components will not de-mix.

In general, we generated some data related to carbonic acid esters in electrolytic solvents, by taking the data from two databases. Apart from that, we validated the data in these databases as well as the proper functionality and adaptability of COSMO-SAC in battery research.



## 7. Further work

The next step after this project would be performing a DFT calculation of some Li electrolytes ( $\text{LiPF}_6$  or  $\text{LiTFSI}$ ) and proceed with the calculation of solubility in the mixtures studied in this project, enthalpies of mixing and other properties that can be derived from activity coefficients. From this starting point, new combinations of solvents can be tested in order to find better mixtures for LIB or even get a suitable mixture for a new electrolyte without measuring experimentally.

Also, in future modifications of the program, someone may probably come up with a solution for the phase changing problem, specifically with gas phase, and thus make COSMO-SAC a fluid phase model instead of just a liquid model.

## 8. References

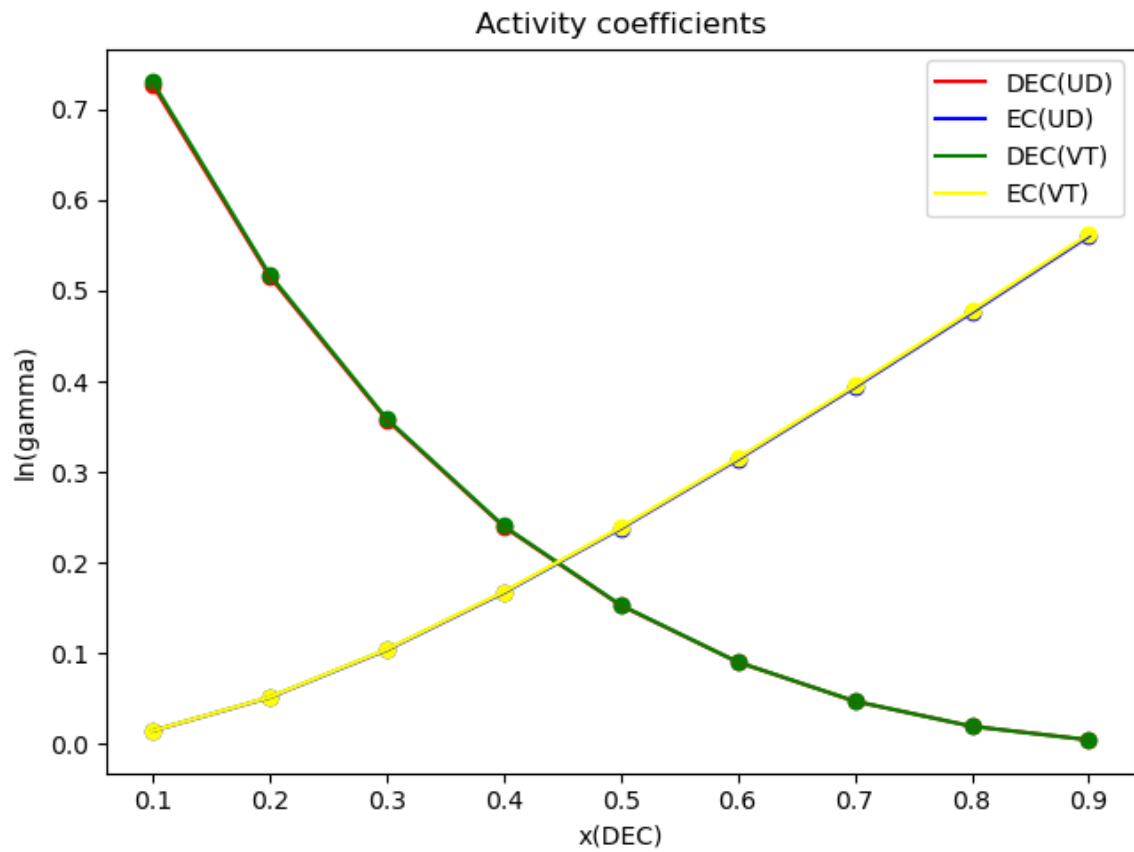
- [1] Klamt, A.; Jonas, V.; Burger, T.; Lohrenz, J. Refinement and Parametrization of COSMO-RS. *J. Phys. Chem* **1998**, A, 102, 5074.
- [2] Lin, S.-T.; Shu Wang, J. C.; Goddard, W. A. and Sandler, S.I. Prediction of Vapor Pressures and Enthalpies of Vaporization Using a COSMO Solvation Model. *J. Phys. Chem.* **2004** A, 108, 7429–7439.
- [3] Wang, S.; Sandler, S. I.; Chen, C.-C. Refinement of COSMO–SAC and the Applications. *Ind. Eng. Chem. Res.* **2007**, 46, 7275–7288
- [4] Lin, S.-T.; Sandler, S. I. A Priori Phase Equilibrium Prediction from a Segment Contribution Solvation Model. *Ind. Eng. Chem. Res.* **2002**, 41, 899–913.
- [5] Hsieh, C.-M.; Sandler, S. I.; Lin, S.-T. Improvements of COSMO-SAC for vapor–liquid and liquid–liquid equilibrium predictions. *Fluid Phase Equilib.* **2010**, 297, 90–97.
- [6] Hsieh, C.-M.; Lin, S.-T.; Vrabec, J. Considering the dispersive interactions in the COSMO-SAC model for more accurate predictions of fluid phase behavior. *Fluid Phase Equilib.* **2014**, 367, 109–116.
- [7] Li, Y.; Chen, X.; Wang, L.; Wei, X.; Nong, M.; Nong, W. and Liang, J.; Measurement and Prediction of Isothermal Vapor–Liquid Equilibrium and Thermodynamic Properties of a Turpentine + Rosin System Using the COSMO-RS Model. *ACS Omega* **2022** 7 (19), 16270-16277
- [8] Bell, I.H.; Mickoleit, E.; Hsieh, C.-M.; Lin, S.-T.; Vrabec, J.; Breitkopf C. and Jäger A. A Benchmark Open-Source Implementation of COSMO-SAC. *Journal of Chemical Theory and Computation* **2020** 16 (4), 2635-2646
- [9] Mullins, E.; Oldland, R.; Liu, Y. A.; Wang, S.; Sandler, S. I.; Chen, C.-C.; Zwolak, M.; Seavey, K. C. Sigma-Profile Database for Using COSMO-Based Thermodynamic Methods. *Ind. Eng. Chem. Res.* **2006**, 45, 4389–4415.
- [10] Mullins, E.; Liu, Y. A.; Ghaderi, A.; Fast, S. D. Sigma Profile Database for Predicting Solid Solubility in Pure and Mixed Solvent Mixtures for Organic Pharmacological Compounds with COSMOBased Thermodynamic Methods. *Ind. Eng. Chem. Res.* **2008**, 47, 1707–1725.
- [11] Schmitz R. Murmann P. Schmitz R. Müller R. Krämer L. Kasnatscheew J. Isken P. Niehoff P. Nowak S. Röschenthaler G. Ignatiev N. Sartori P. Passerini S. Kunze M. Lex-Balducci A. Schreiner C. Cekic-Laskovic I. Winter M. Investigations on novel electrolytes, solvents and SEI additives for use in lithium-ion batteries: Systematic electrochemical characterization and detailed analysis by spectroscopic methods. *Progress in Solid State Chemistry* **2014**, 65-84, 42(4).
- [12] Wang, S.; Song, Y.; Chen, C.-C. Extension of COSMO-SAC Solvation Model for Electrolytes. *Ind. Eng. Chem. Res.* **2011**, 50, 176–187.
- [13] Uchida S. Kiyobayashi T. What differentiates the transport properties of lithium electrolyte in ethylene carbonate mixed with diethylcarbonate from those mixed with dimethylcarbonate? *Journal of Power Sources*, (2021), 511

- [14] National Institute of Standards and Technology <https://www.nist.gov/> (20/12/2022)
- [15] Hsieh, C.-M.; Lin, S.-T. A predictive model for the excess gibbs free energy of fully dissociated electrolyte solutions *AIChE Journal* **2011**, 57 (4), 1061-1074.
- [16] Soares, R. P.; Staudt, P.B.; Beyond activity coefficients with pairwise interacting surface (COSMO-type) models *Fluid Phase Equilibria* **2022**, 564, 113611
- [17] Diedenhofen, M.; Klamt, A. COSMO-RS as a tool for property prediction of IL mixtures—A review *Fluid Phase Equilibria* **2010**, 294 (1-2) 31-38
- [18] Islam, M.R.; Chen, C.C.; COSMO-SAC Sigma Profile Generation with Conceptual Segment Concept *Ind. Eng. Chem. Res.* **2015** 54 (16) 4441-4454
- [19] Dong, Y.; Huang, S.; Guo, Y.; Lei, Z.; COSMO-UNIFAC model for ionic liquids *AIChE J* **2020** 66 (1)
- [20] Ding, M. S.; Excess Gibbs Energy of Mixing for Organic Carbonates from Fitting of Their Binary Phase Diagrams with Nonideal Solution Models *J Solution Chem* **2005** 34 (3) 343-359
- [21] Ferro, V. R.; Palomar, J.; Ortega, J.; Rodríguez, J. J.; Interactions of Ionic Liquids and Acetone: Thermodynamic Properties, Quantum-Chemical Calculations, and NMR Analysis *J. Phys. Chem.* **2013** B 117 (24) 7388-7398
- [22] Ding, M.S.; Xu, K.; Zhang, S.; Jow, T. R.; Liquid/Solid Phase Diagrams of Binary Carbonates for Lithium Batteries Part II *J. Electrochem. Soc.* **2001** 148 (4) A299
- [23] Scrosati, B.; Hassoun, J.; Sun, Y. -K.; Lithium-ion batteries. A look into the future *Energy Environ.* **2011** Sci. 4(9) 3287
- [24] Mahmoudabadi, S.; Pazuki, G.; Modelling of thermodynamics properties of amino acid solutions by COSMO-SAC model *Fluid Phase Equilibria* **2021** 541, 113078
- [25] Xu, K.; Nonaqueous Liquid Electrolytes for Lithium-Based Rechargeable Batteries *Chem. Rev.* **2004** 104 (10) 4303-4418
- [26] Yu, G.; Wei, Z.; Chen, K.; Guo, R.; Lei, Z.; Predictive molecular thermodynamic models for ionic liquids *AIChE Journal* **2022** 68 (4)
- [27] Hassoun, J.; Scrosati, B.; Review—Advances in Anode and Electrolyte Materials for the Progress of Lithium-Ion and beyond Lithium-Ion Batteries *J. Electrochem. Soc.* **2015** 162 (14) A2582-A2588
- [28] Champion, C.; Li, W.; Lucht, B. L.; Thermal Decomposition of LiPF<sub>6</sub>-Based Electrolytes for Lithium-Ion Batteries **2005** 152 (12) A2327
- [29] Wang, S.; Lin, S.-T.; Watanasiri, S.; Chen, C.-C.; Use of GAMESS/COSMO program in support of COSMO-SAC model applications in phase equilibrium prediction calculations *Fluid Phase Equilibria* **2009** 276 (1) 37-45
- [30] Kim, S.; Bang, J.; Yoo, J.; Shin, Y.; Bae, J.; A comprehensive review on the pretreatment process in lithium-ion battery recycling *Journal of Cleaner Production* **2021** 294, 126329
- [31] Lide, D. R.; *Handbook of organic solvents* CRC press **1995**
- [32] Atkins, P.; Friedman R.; *Molecular quantum mechanics*, Oxford University Press, fifth edition, **2011**

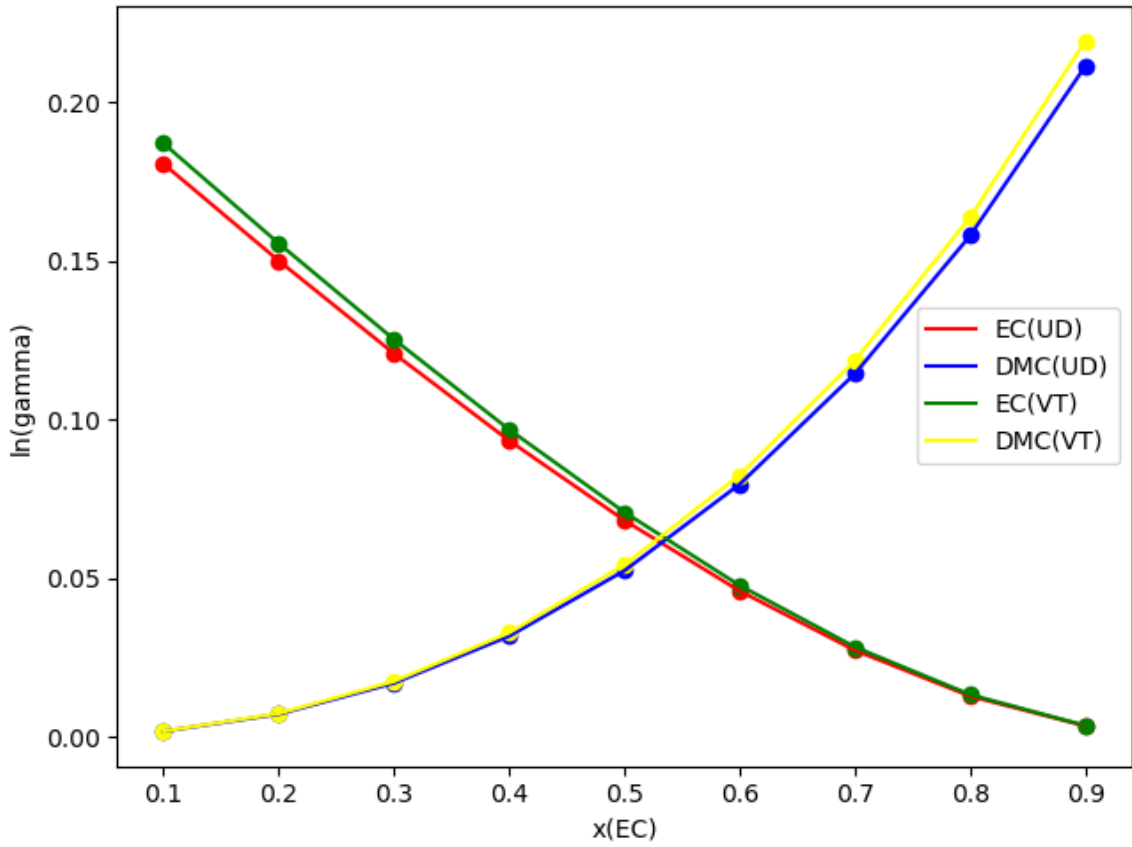
- [33] David E.; Woon and Thorn H.; Dunning, Jr.; Gaussian basis sets for use in correlated molecular calculations. III. The atoms aluminum through argon; *J. Chem. Phys.* **1993** 98 (2)
- [34] Herre W. J.; Stewart R. F.; Pople J. A.; Self-Consistent Molecular-Orbital Methods. I. Use of Gaussian Expansions of Slater-Type Atomic Orbitals *J. Chem. Phys.* **1969** 51, 2657–2664
- [35] Ditchfield R.; Hehre W. J.; Pople J. A. Self-Consistent Molecular Orbital Methods. IX. An Extended Gaussian Type Basis for Molecular - Orbital Studies of Organic Molecules *J. Chem. Phys.* **1971** 54, 724–728
- [36] Dunning T. H., Jr. Gaussian basis sets for use in correlated molecular calculations. I. The atoms boron through neon and hydrogen *J. Chem. Phys.* **1989** 90, 1007–1023
- [37] Becke, A. D.; Density-functional exchange-energy approximation with correct asymptotic behavior, *Phys. Rev. A* **1988** 38 (6)
- [38] Lee C., Yang W., Parr R. G.; Development of the Colle-Salvetti correlation-energy formula into a functional of the electron density, *Phys. Rev. B* **1988** 37 (2)
- [39] Grimme S., Ehrlich S., Goerigk L. Effect of the Damping Function in Dispersion Corrected Density Functional Theory, *J Comput Chem* **2011** 32: 1456–1465
- [40] Grimme S. Semiempirical hybrid density functional with perturbative second-order correlation, *J. Chem. Phys.* **2006** 124, 034108
- [41] Gaussian 16, M. J. Frisch et. al. Revision A.03 **2016**
- [42] Grimme S., Antony J., Ehrlich S., Krieg H., A consistent and accurate *ab initio* parameterization of density functional dispersion correction (DFT-D) for the 94 elements H-Pu *J. Chem. Phys.*, **2010** 132, 154104.

## 9. Appendices

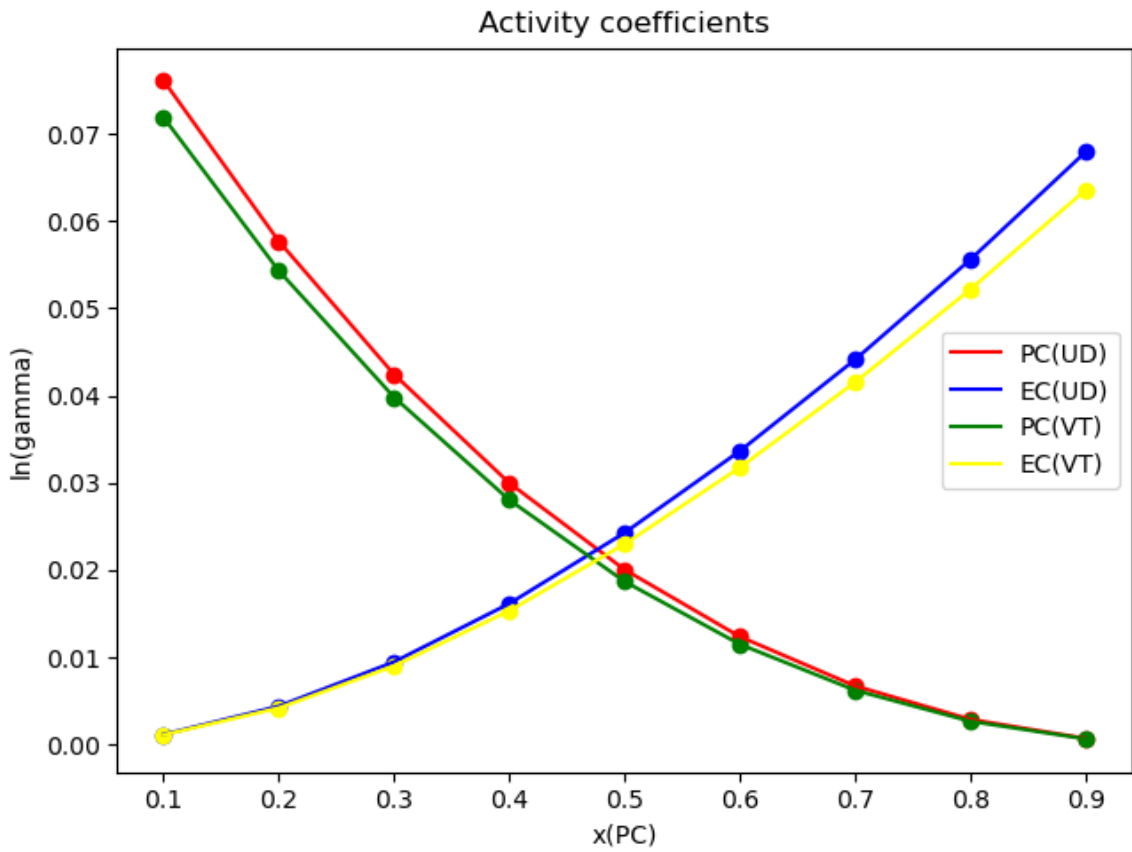
### Appendix A: Activity coefficient profiles



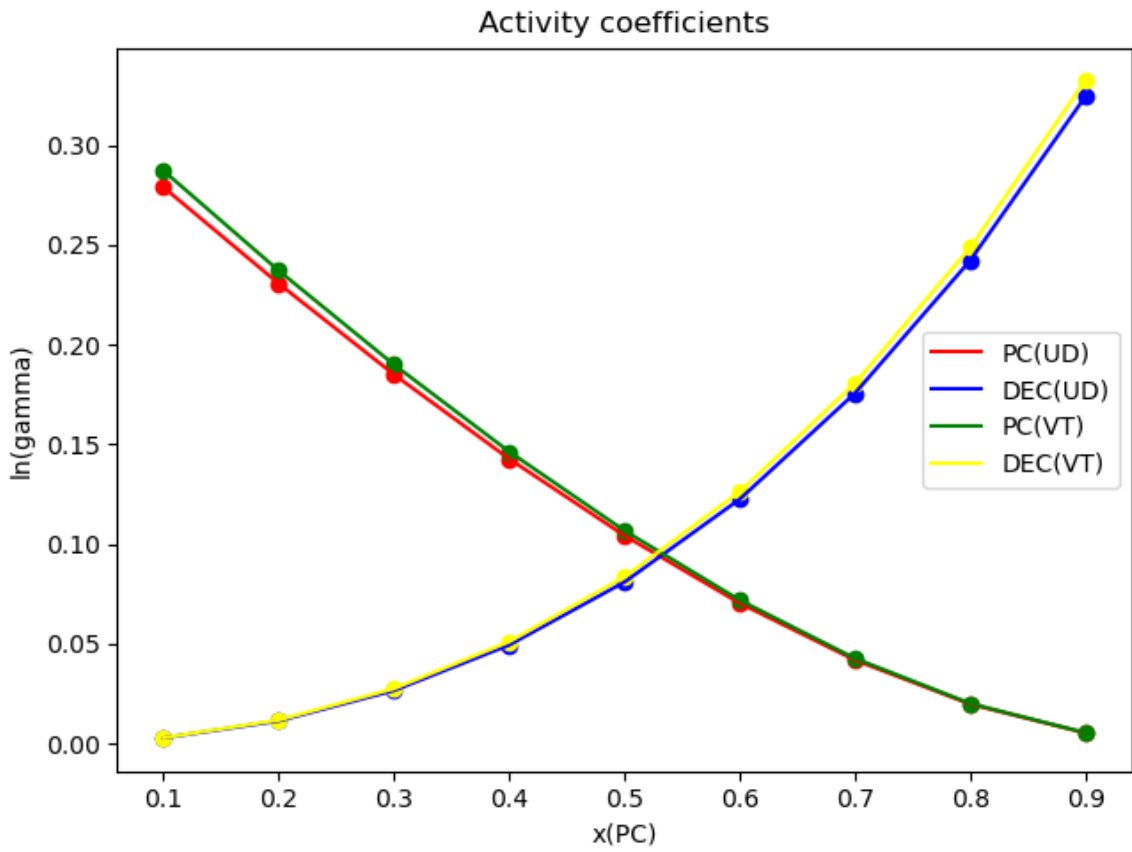
A1. Activity coefficients for EC+DEC



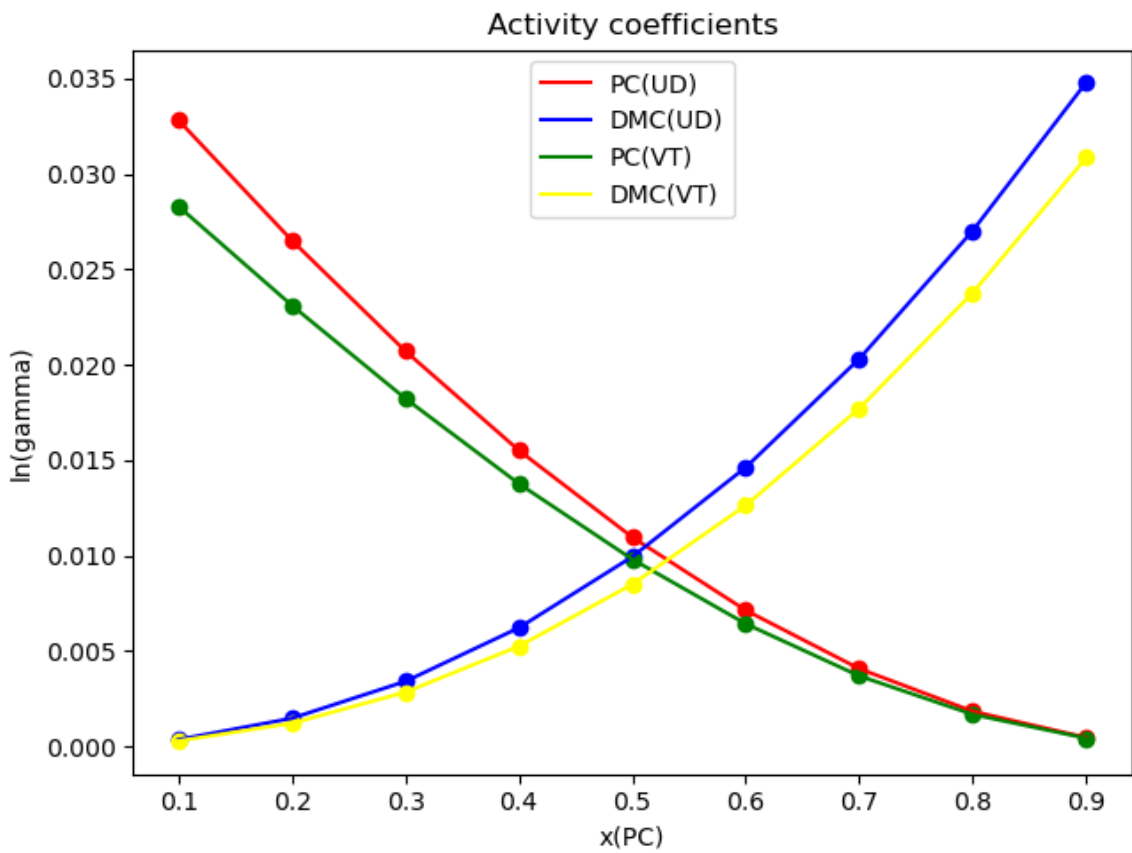
A2. Activity coefficients for EC+DMC



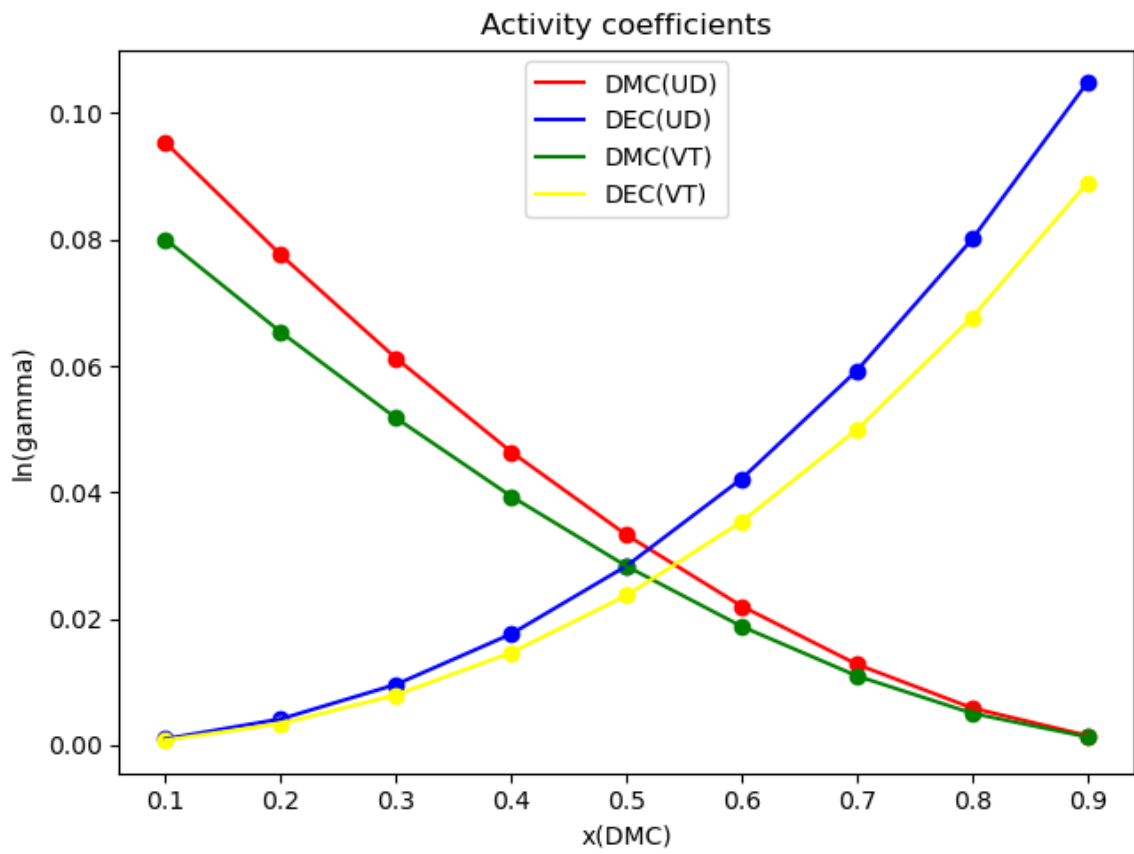
A3. Activity coefficients for PC+EC



A4. Activity coefficients for PC+DEC



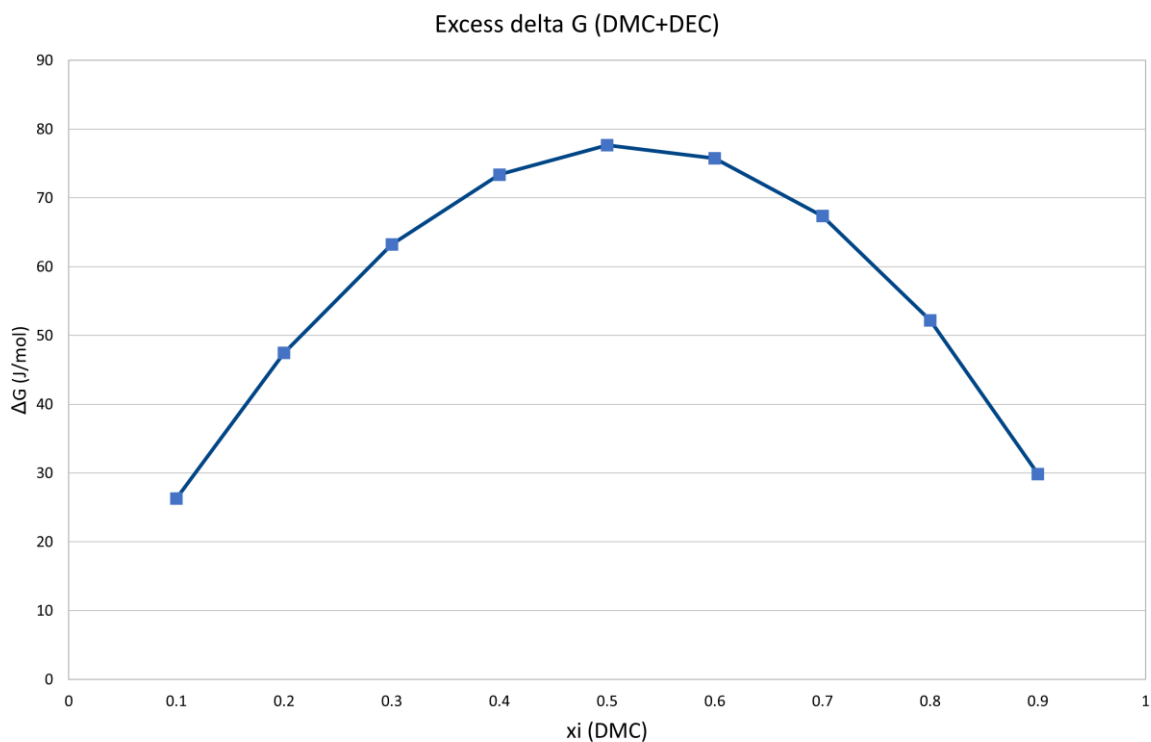
A5. Activity coefficients for PC+DMC



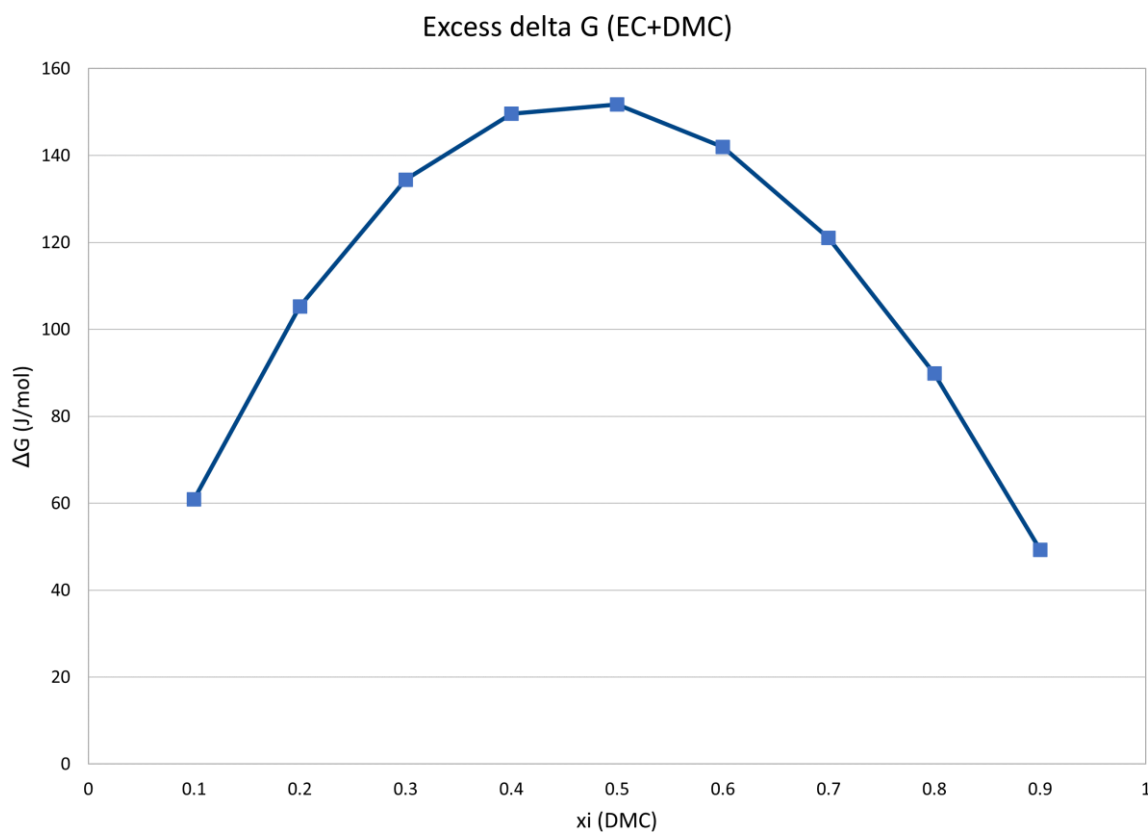
A6. Activity coefficients for DMC+DEC



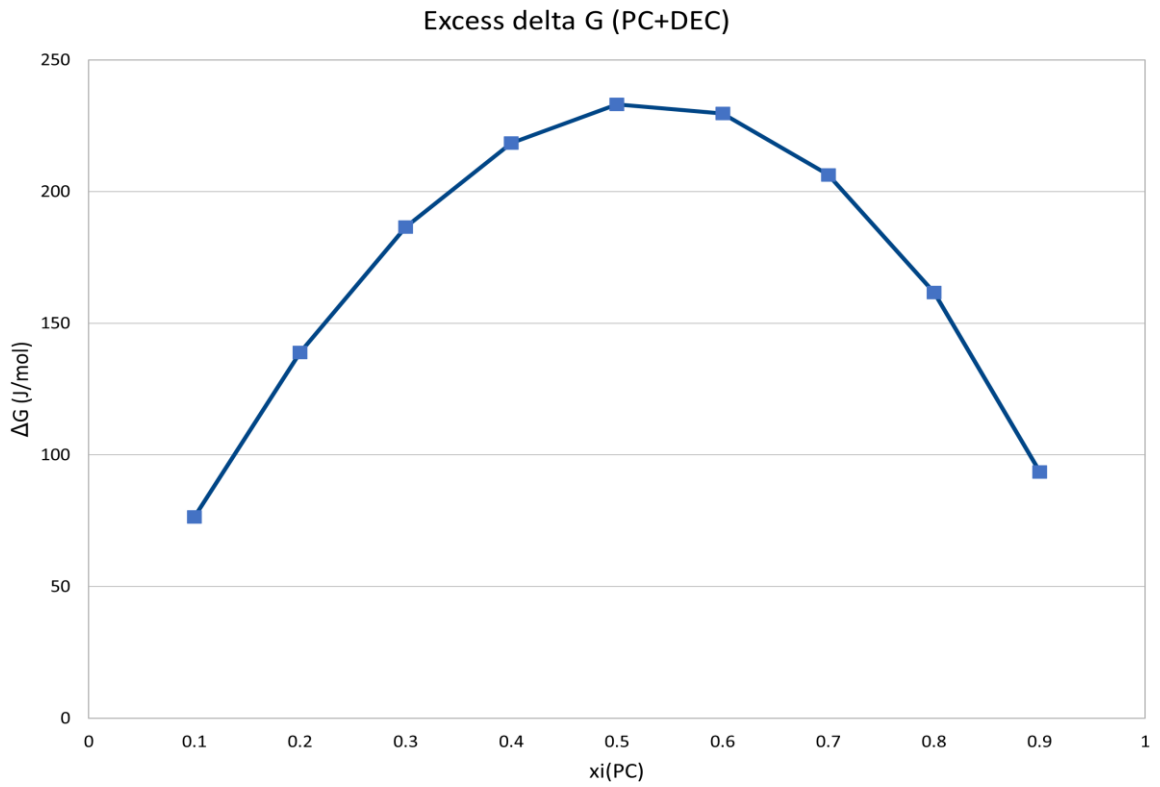
## Appendix B-Excess free energy of mixing



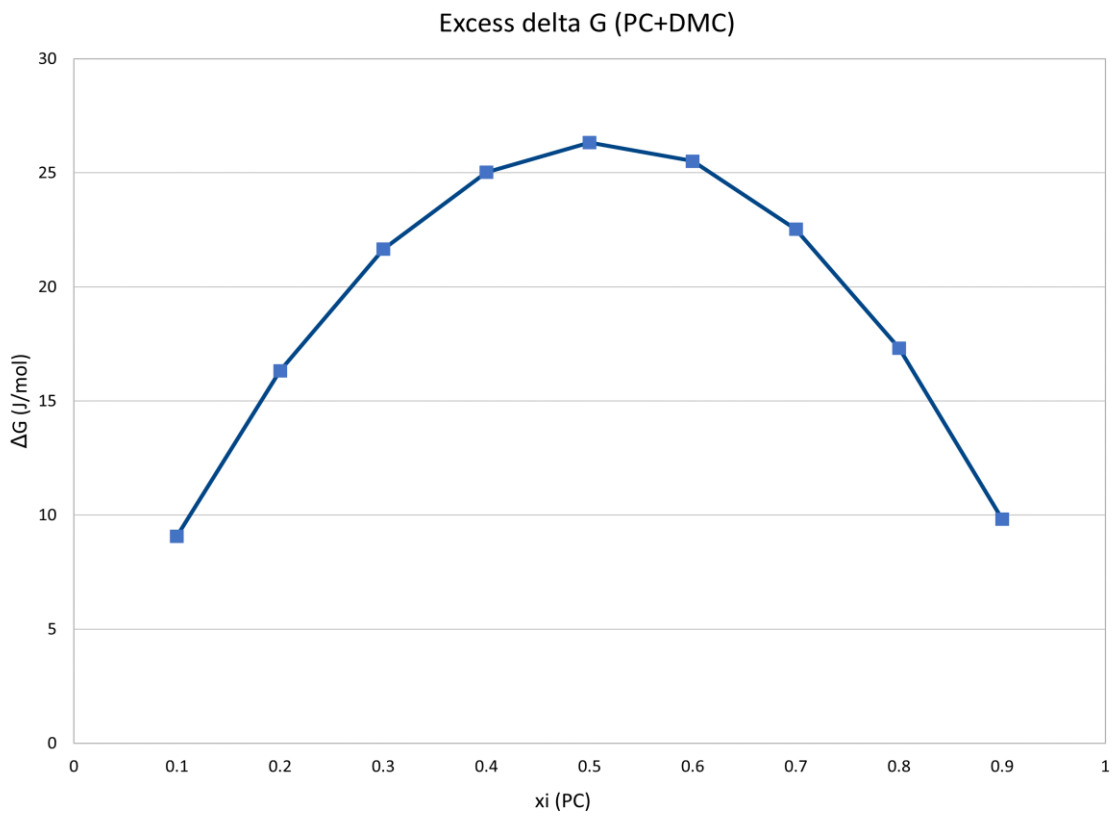
*B1. Excess free energy for DMC+DEC*



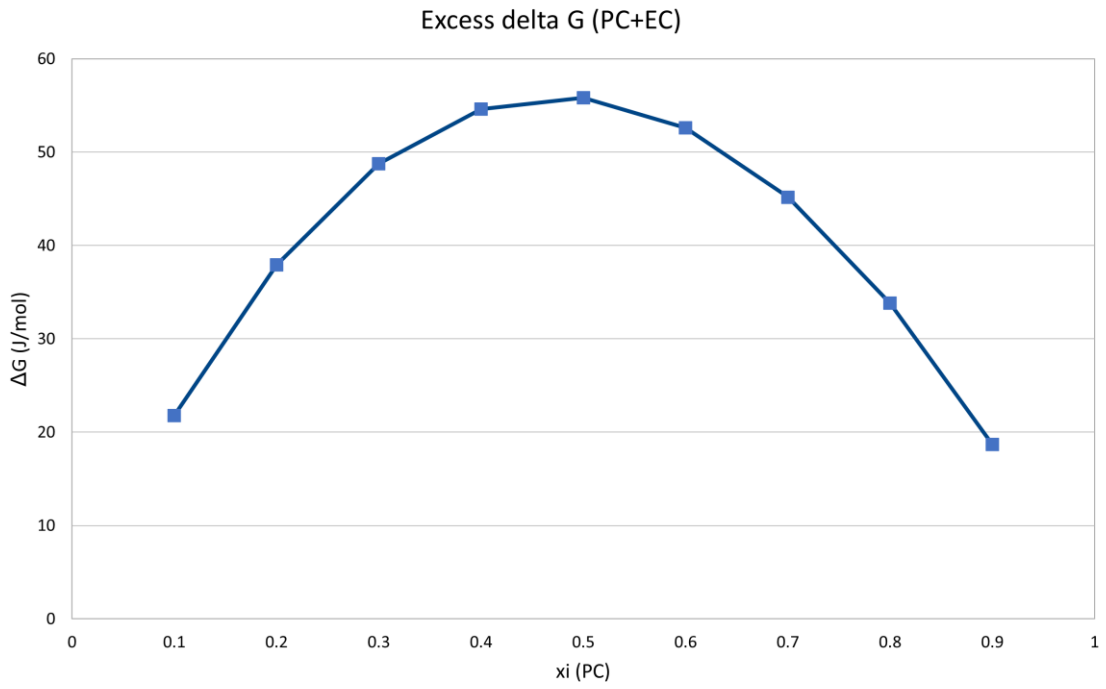
*B2. Excess free energy for EC+DMC*



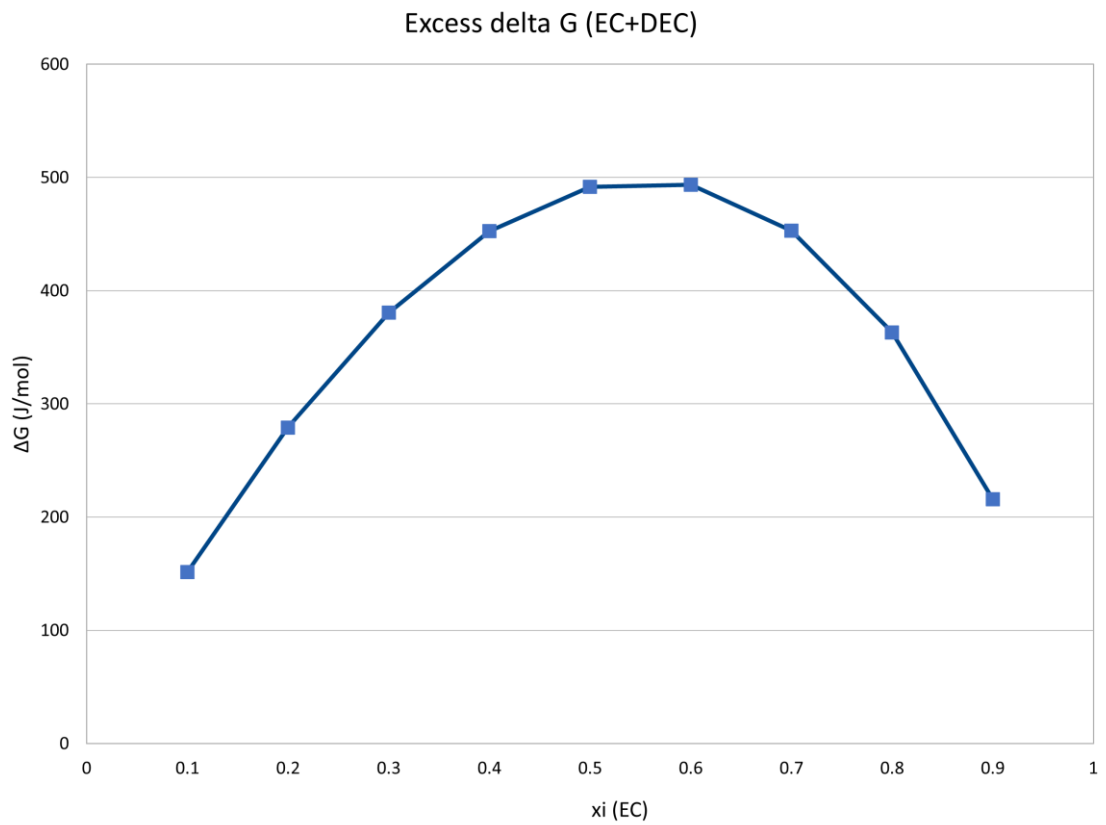
*B3. Excess free energy for PC+DEC*



*B4. Excess free energy for PC+DMC*

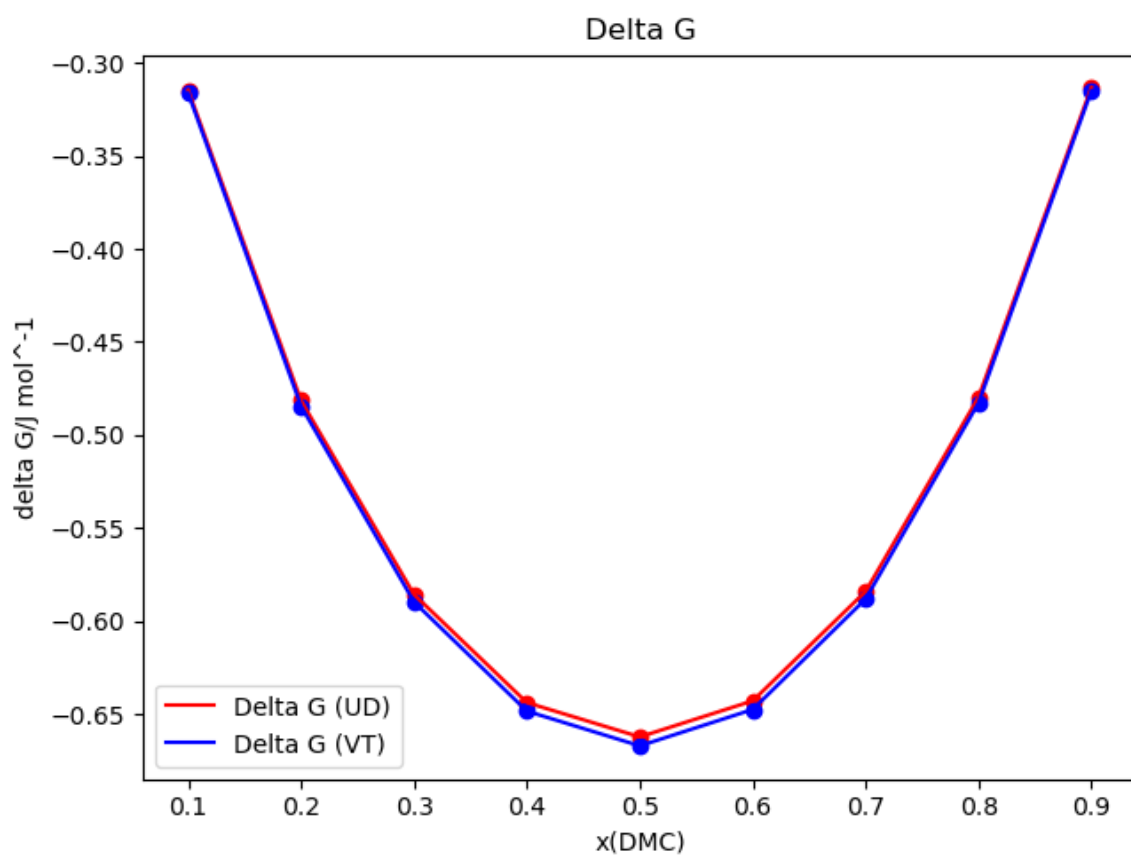


*B5. Excess free energy for PC+EC*

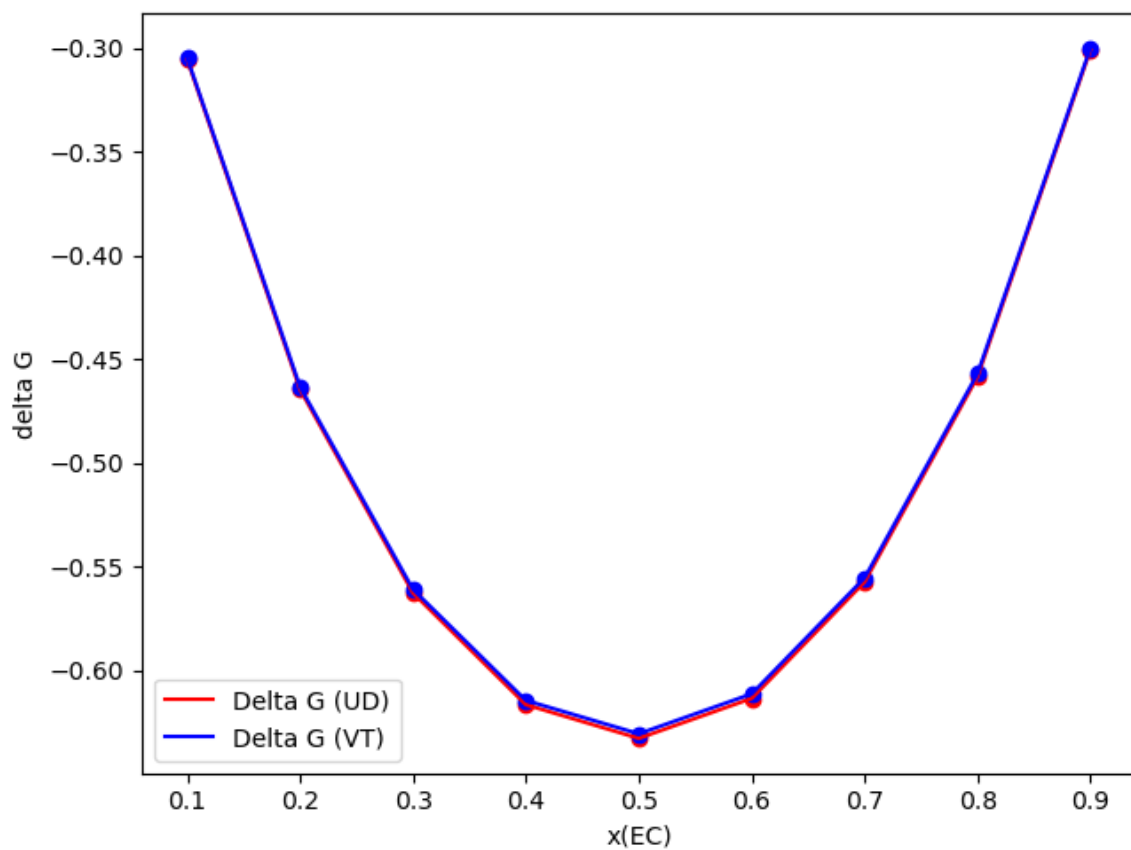


*B6. Excess free energy for EC+DEC*

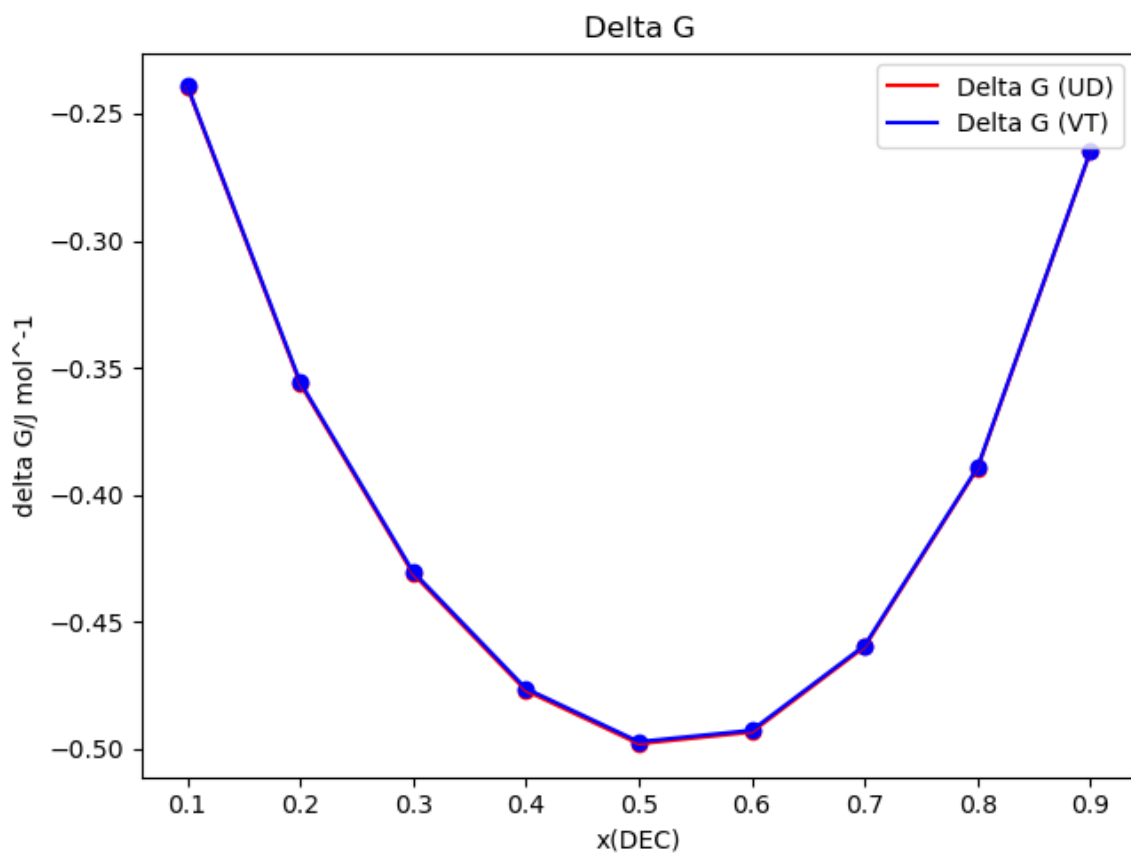
## Appendix C: Gibbs free energy of mixing



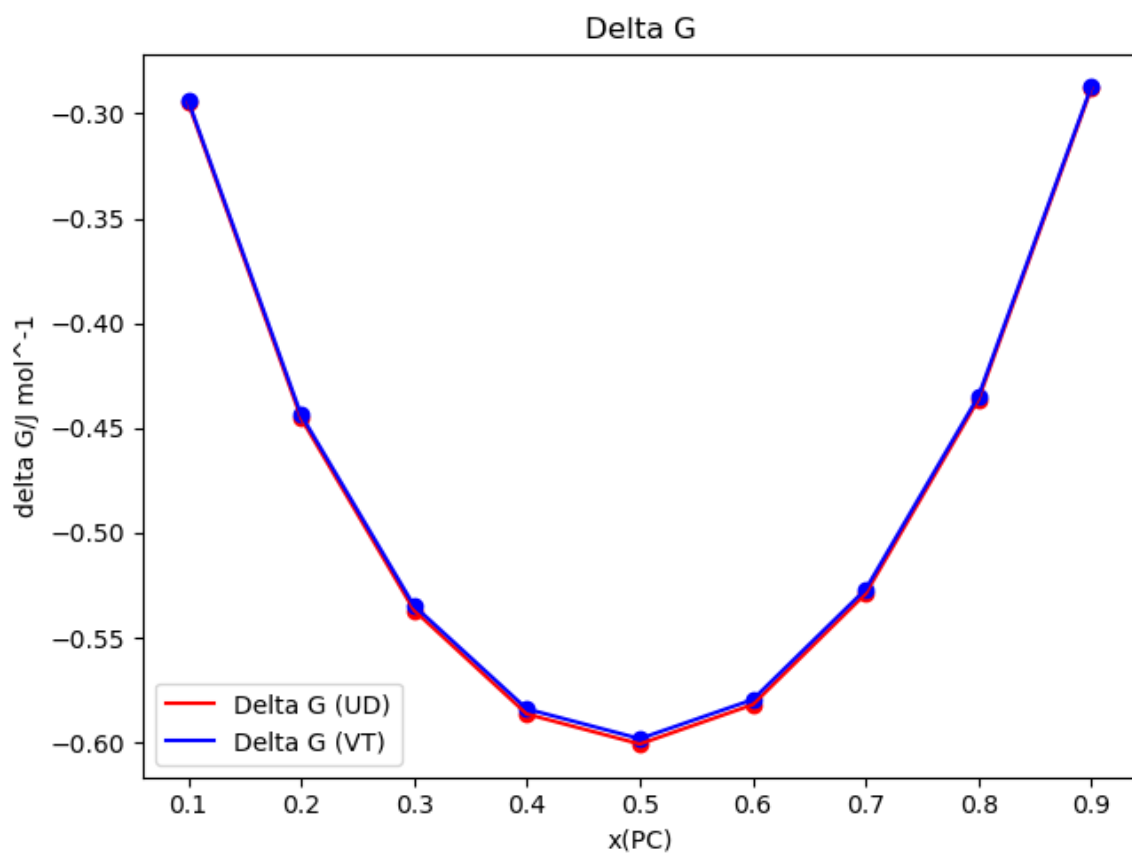
C1. Free energy of mixing for DMC+DEC



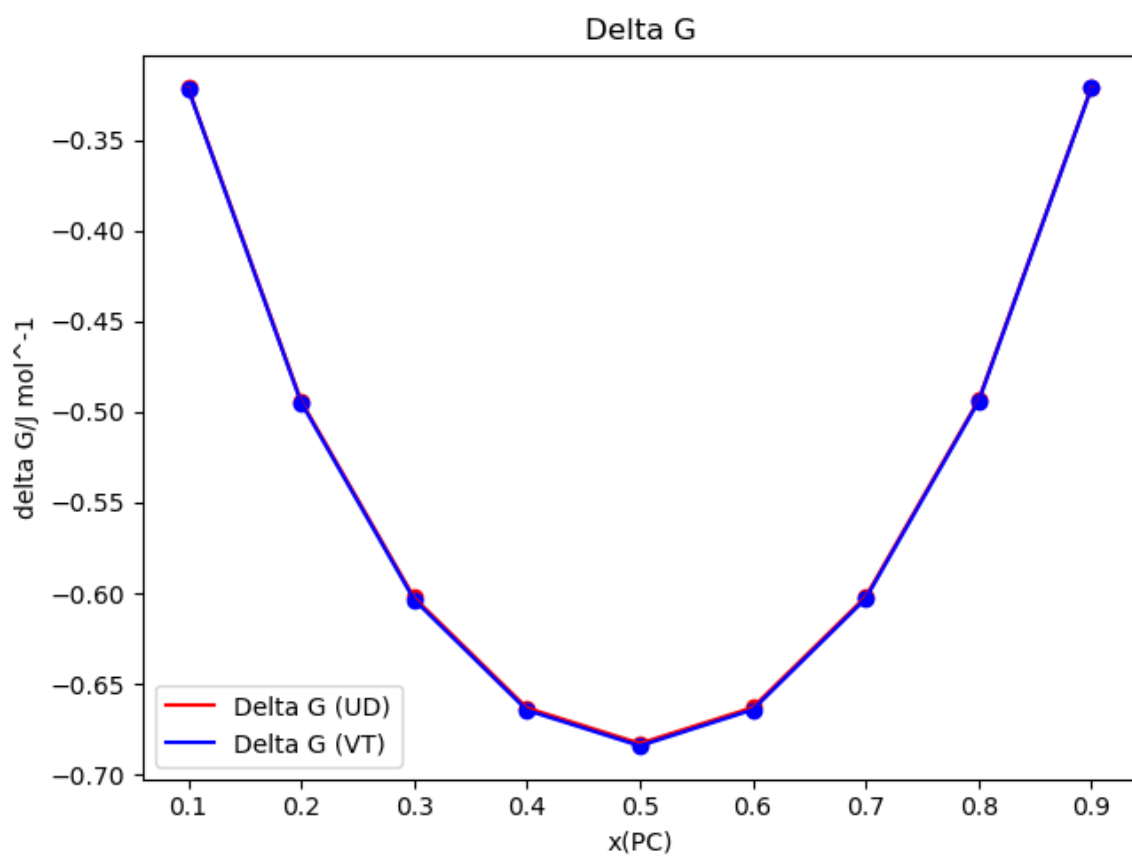
C2. Free energy of mixing for EC+DMC



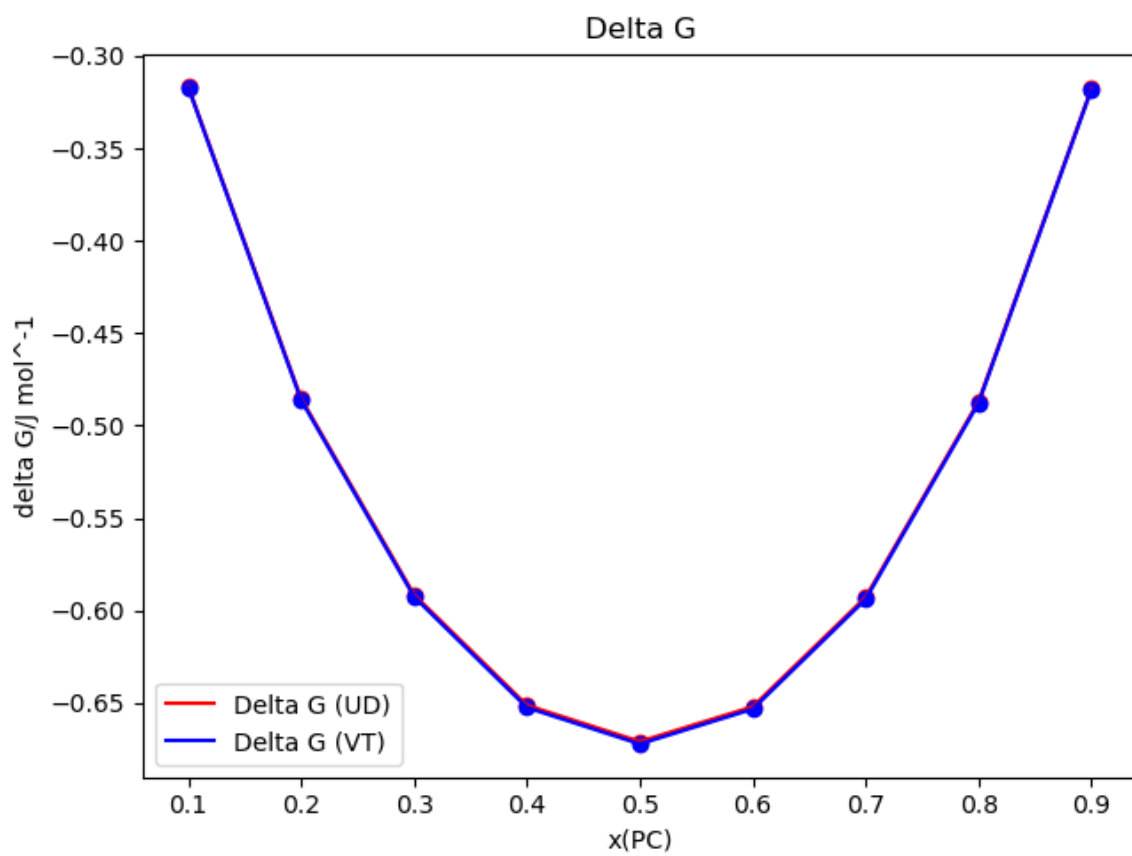
C3. Free energy of mixing for EC+DEC



*C4. Free energy of mixing for PC+DEC*

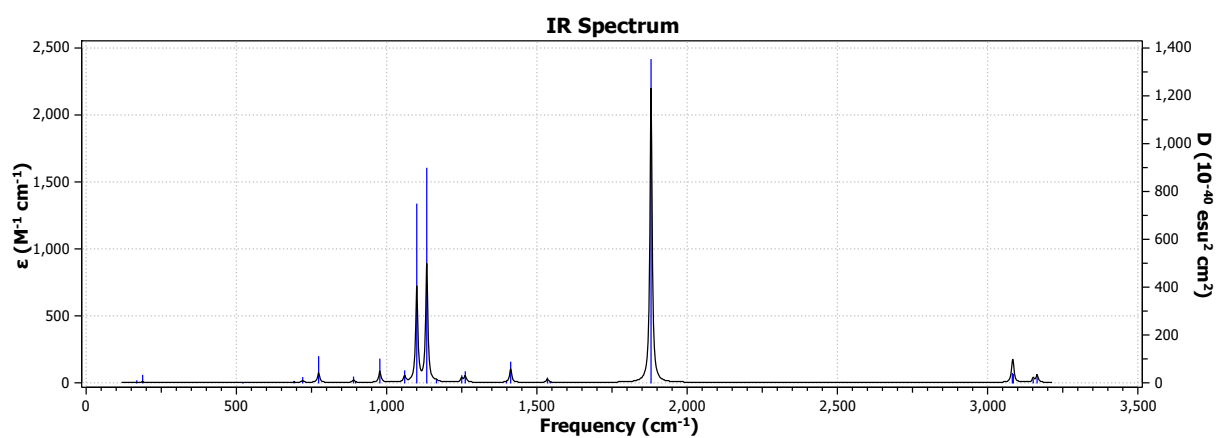


*C5. Free energy of mixing for PC+DMC*

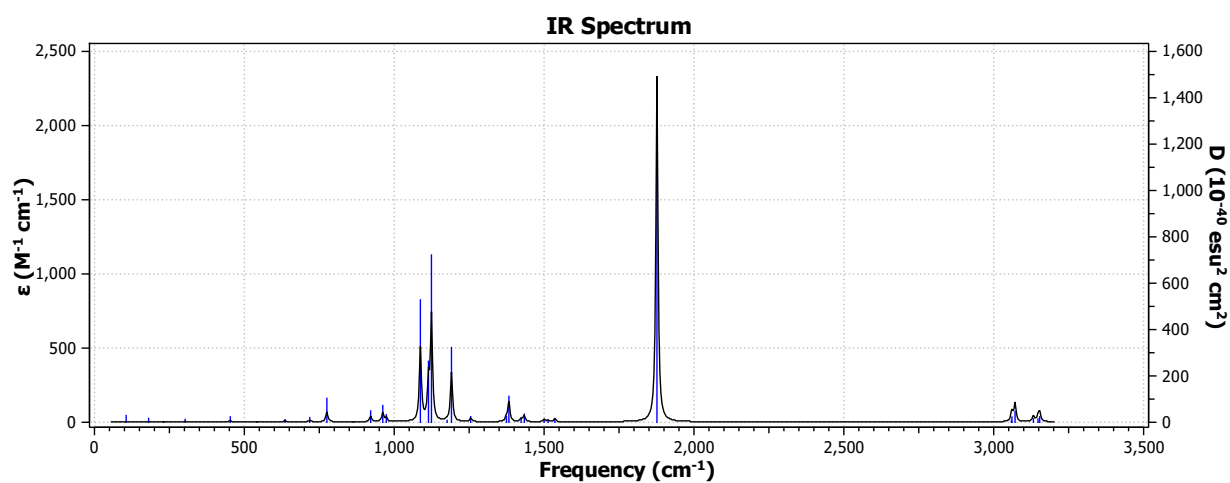


C6. Free energy of mixing for EC+PC

## Appendix D: Infrared vibrational spectra

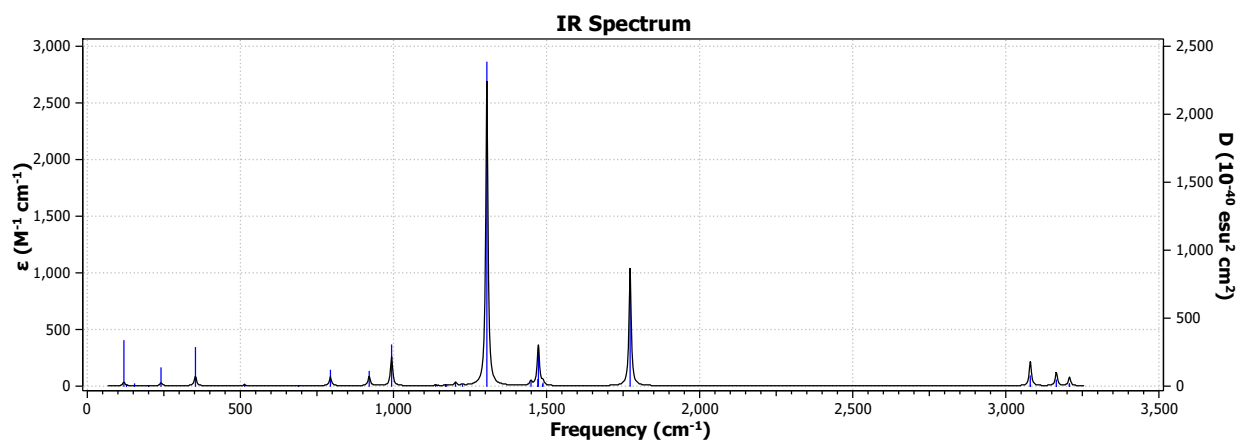


*D1. IR spectra of EC*

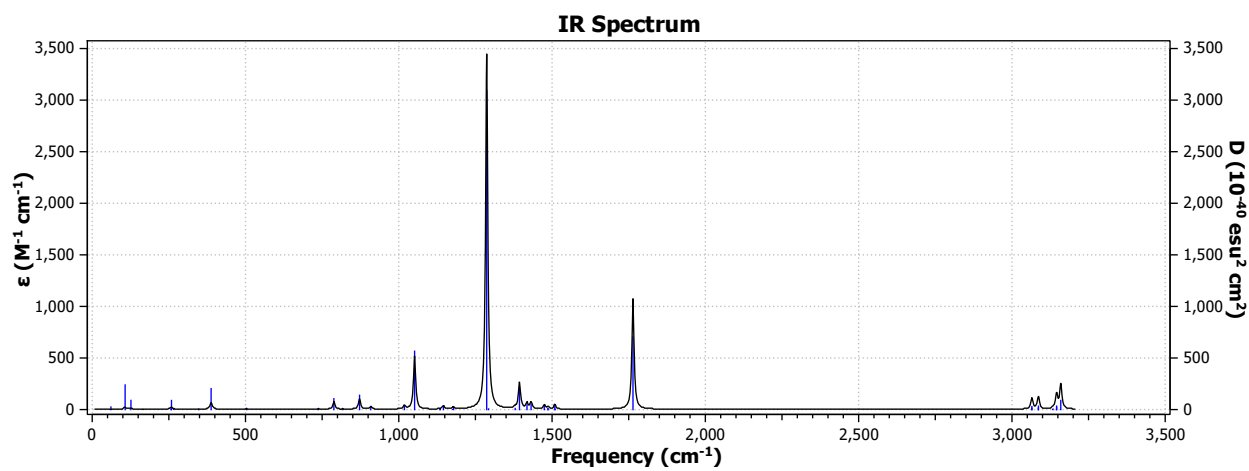


*D2. IR spectra of PC*



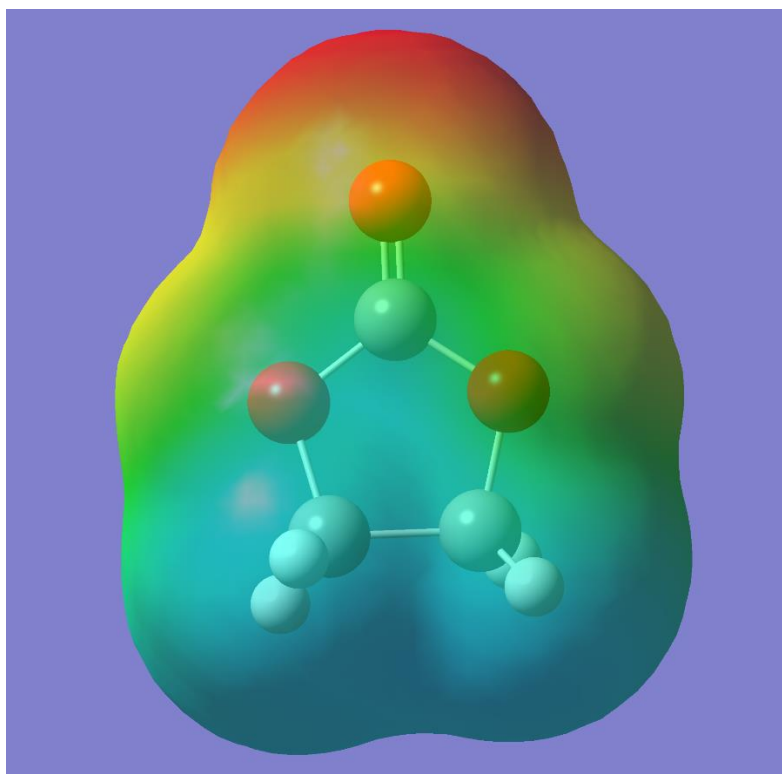


*D3. IR spectra of DMC*

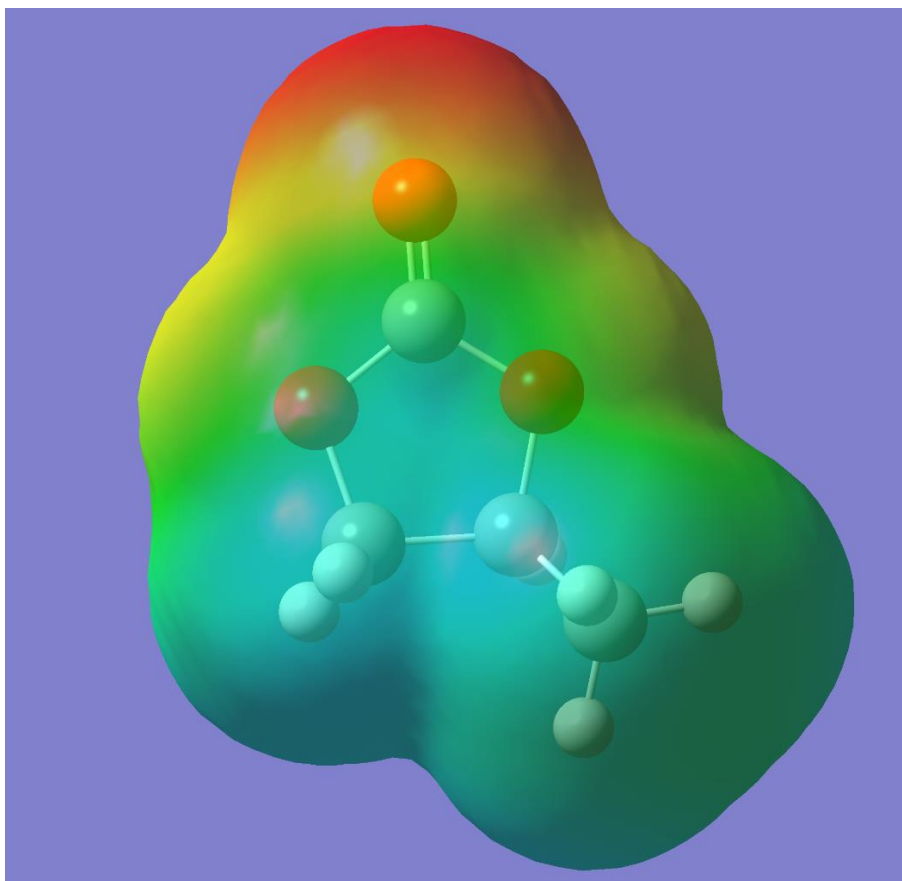


*D4. IR spectra of DEC*

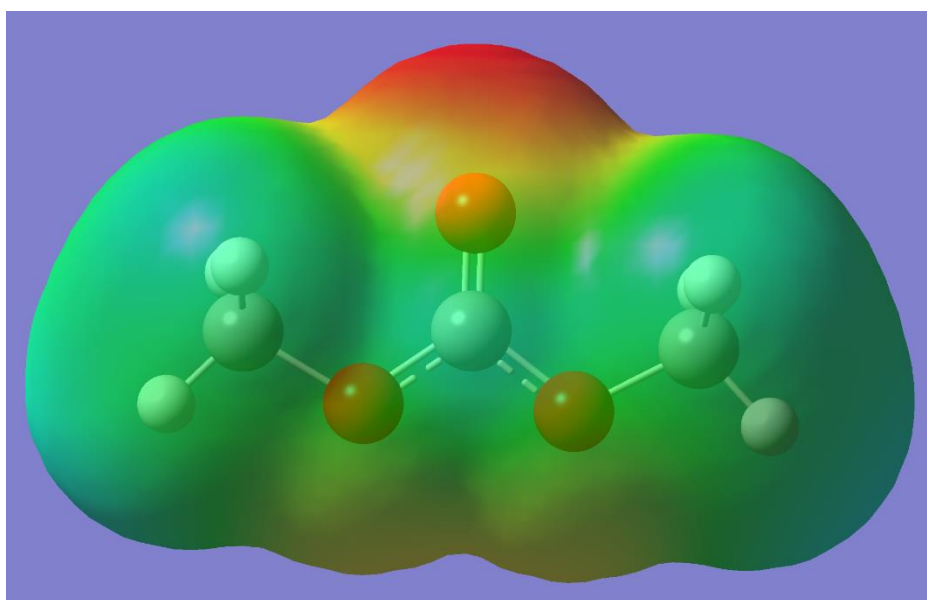
## Appendix E: Electrostatic potential surfaces



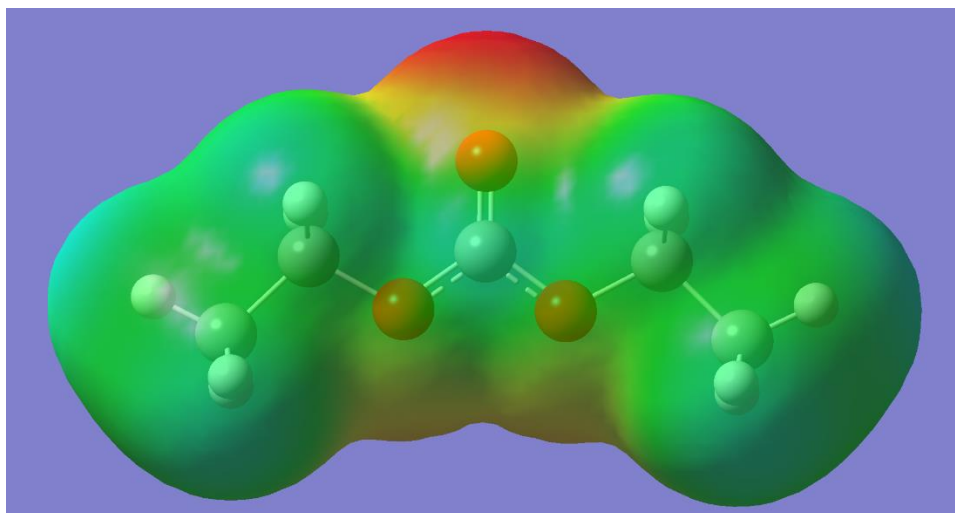
*E1. Electrostatic potential of EC*



*E2. Electrostatic potential of PC*



*E3. Electrostatic potential of DMC*



*E4. Electrostatic potential of DEC*

---